TURUN YLIOPISTO

Structural interpretation of the Iso-Kuotko area, Lapland, with implications to gold precipitation

Bedrock geology

Master's thesis

Author:

Olli Silvonen

20.12.2023

Turku

Master's thesis

Subject: Bedrock geology
Author: Olli Silvonen
Title: Structural interpretation of the Iso-Kuotko area, Lapland, with implications to gold precipitation
Supervisor: Pietari Skyttä
Number of pages: 56 pages + 7 appendix pp.
Date: 20.12.2023

Central Lapland Belt (CLB) in Northern Finland hosts multiple orogenic gold deposits from which Iso-Kuotko gold deposit is one. The Iso-Kuotko deposit comprises three mineralizations: Kati, Retu and Tiira. Previous studies have focused on the geochronology and geochemical attributes of the deposit, whereas the structural geometry of the deposit, and the linkage between gold-bearing veins and shear features remains partly unknown. The main goal of this study is to describe both the ductile and brittle deformation structures of the study area and to link them together. The secondary objective is to identify and compare the orientations distribution of diverse vein sets occurring within the mineralized areas, and further compare them with the mineralization. The study is based on new field observations and structural measurements from drill core and bore hole videos, which complement the pre-existing datasets available from several parts of the study area. Moreover, a structural interpretation of magnetic anomaly maps was conducted, and previously gathered drill core measurements were used in the study. The data were eventually gathered into digital 3D models and lower hemisphere projections. The Kati area is dominated by gently NE dipping foliation which has been sheared during a thrusting event. The Kati area is also cross-cut by NW trending, likely dextral, sub-vertical shear bands splaying out from the Kiistala Shear Zone (KiSZ). Additionally, in the Kati area there is a E-W trending, sub-vertical, shear band possibly splaying out from the NW trending shear bands. The Retu area is dominated by sub-horizontal foliation which is undulating around gently NE plunging fold axis. According to this study, shear deformation occurred along the sub-horizontal foliation surface, and the foliation was cross-cut by the main branch of the NE trending sub-vertical KiSZ and parallel subsidiary shear bands. In total five mineralogically varying vein types were observed: 1) quartz, 2) quartz + Fe-carbonate, 3) quartz + Fe-carbonate + sulphide, 4) calcite and 5) quartz + calcite. All of the shear features in both Kati and Retu areas contain the gold-critical type 3 (quartz + Fe-carbonate + sulphide) veins. The veining is mainly controlled by shear features as well as competent lithologies, including felsic dykes and albite + sericite altered mafic volcanic rocks. In comparison, the sub-vertical gold-critical veins in the Kati area trend ENE-WSW and NW-SE, whereas the gold-critical veins in the Retu area trend NE-SW.

Keywords: structural geology, orogenic gold, Central Lapland Greenstone Belt, 3D modelling

Pro gradu -tutkielma

Oppiaine: Kallioperägeologia
Tekijä: Olli Silvonen
Otsikko: Rakennegeologinen tulkinta Iso-Kuotkon alueesta Lapissa ja rakenteiden vaikutus kullan rikastumiseen
Ohjaaja: Pietari Skyttä
Sivumäärä: 56 sivua + 7 liites.
Päivämäärä: 20.12.2023

Iso-Kuotko on yksi useasta Keski-Lapin vihreäkivivyöhykkeellä sijaitsevasta orogeenisesta kultaesiintymästä. Iso-Kuotkon kultaesiintymä koostuu kolmesta mineralisaatiosta: Kati, Retu ja Tiira. Aiemmat tutkimukset alueelta ovat keskittyneet pääosin alueen geokronologian ja geokemian selvittämiseen. Alueen rakennegeologinen geometria sekä kultapitoisten juonten ja hiertorakenteiden yhteys toisiinsa on osittain epäselvä. Tutkimuksen tavoitteena on i) kuvailla Iso-Kuotkon duktiileja ja hauraita deformaatiorakenteita ja yhdistää niitä toisiinsa, ja ii) tunnistaa mineralogialtaan erilaisia juonia ja verrata niiden orientaatioita toisiinsa sekä eri mineralisaatioiden välillä. Tutkimusaineisto koostuu jo olemassa olevan aineiston lisäksi uusista kenttähavainnoista, kairasydänten ja optisesti kuvattujen kairareikien rakennemittauksista sekä aeromagneettisen kartan perusteella tehdystä rakennetulkinnasta. Aineistosta koostettiin 3D-malli ja alapalloprojektioita. Kati alueen liuskeisuus on loivaa kaatuen pääosin koilliseen. Liuskeisuus on hiertynyt koilliseen kaatuvan ylityöntövyöhykkeen vaikutuksesta. Kati alueen liuskeisuutta leikkaa luoteissuuntaiset, todennäköisesti oikeakätiset, lähes pystysuorat hiertosaumat. Luoteissuuntaiset hiertosaumat erkanevat Kiistalan hiertovyöhykkeestä (KiSZ). Kati alueen itä-länsi suuntaiset lähes pystysuorat hiertosaumat erkanevat todennäköisesti luoteissuuntaisista hiertosaumoista. Retu alueen liuskeisuus on pääosin lähes horisontaalia. Liuskeisuus unduloi loivasti koilliseen kaatuvan poimuakselin ympärillä. Tämän tutkimuksen mukaan lähes horisontaali liuskeisuus on hiertynyt ja liuskeisuutta leikkaa lähes pystysuora koillisen suuntainen KiSZ ja sen toissijaiset hiertosaumat. Tutkimuksessa havaittiin viisi mineralogisesti poikkeavaa juonta: 1) kvartsi, 2) kvartsi + Fe-karbonaatti, 3) kvartsi + Fe-karbonaatti + sulfidi, 4) kalsiitti, ja 5) kvartsi + kalsiitti. Kaikki Kati ja Retu alueiden hiertorakenteet sisältävät kultakriittistä juoni tyyppiä 3 (kvartsi + Fe-karbonaatti + sulfidi). Hiertorakenteet ja kompetentit felsiset juonet ja albiitti + serisiitti muuttuneet mafiset vulkaniitit kontrolloivat juonitusta. Kati alueen lähes pystysuorat kultakriittiset juonet ovat suunnaltaan pääosin ENE-WSW ja luoteinen-kaakko, kun taas Retu alueen lähes pystysuorat kultakriittiset juonet ovat suunnaltaan koillinen-lounas.

Avainsanat: rakennegeologia, orogeeninen kulta, Keski-Lapin vihreäkivivöyhyke, 3D mallinnus

Table of Contents

1. Introduction

1.1 Study area and exploration history

The study area is located in Central Lapland Belt (CLB), approximately 70 km northeast of Kittilä town and 18 km north of the Suurikuusikko gold mine (Figure 1). The mine is operated by Agnico Eagle Finland Oy. Besides the main deposit, Suurikuusikko, several mineralizations have been studied in the area, Iso-Kuotko is one of them. Mineralizations within the Iso-Kuotko were found by exploration team from Geological Survey of Finland (GTK), managed by FM Ilkka Härkönen in 1986. GTK chose the area for studies by its location within Central Lapland Belt greenstones, close proximity of younger granitic intrusions, signatures within the geophysical low-altitude maps, and bottom of the till analyses (Härkönen, 1994). GTK field team conducted several geophysical investigations including: Slingram, magnetic anomaly, electromagnetic anomaly, VLF-R, and induced polarization measurements, between 1988 and 1992 (Härkönen, 1994). They also excavated numerous research trenches and bottom of the till (BOT) surveys and percussion drilling during the same time period (Härkönen, I, et al., 2000). Additionally, total of 79 diamond drill holes and 14 reverse circulation holes were drilled between 1987 and 1999. GTK studies revealed four gold mineralizations in the Iso-Kuotko area; Kati, Retu, Tiira and Nimetön (Härkönen, I. et al., 2000). A feasibility study for small-scale mining project was completed in 1997, but metallurgical tests showed too low gold yield for economic mining.

Later in 2001 Riddarhyttan AB bought Iso-Kuotko deposit from GTK and continued diamond drilling and geophysical surveys in the Iso-Kuotko area. The Iso-Kuotko gold mineralizations have been explored by Agnico Eagle Finland Oy (AEF) since 2006.

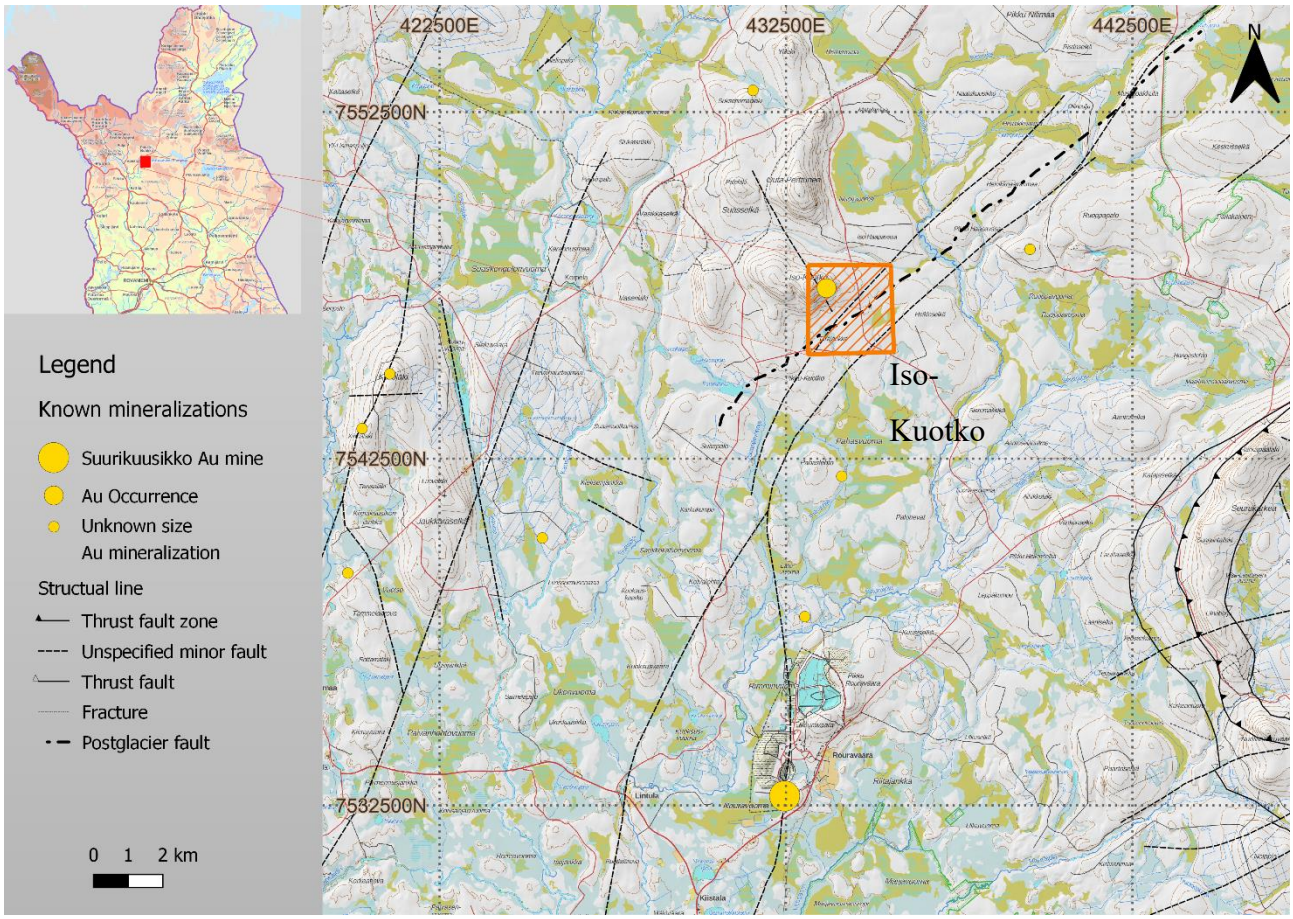

Figure 1. Map of the study area. Base map from MML (Maanmittauslaitos), known mineralizations and structural trend lines from GTK data.

Iso-Kuotko is dominated by Fe-rich tholeiitic tuffs, lavas, and pyroclastic rocks as well as felsic porphyry veins and both felsic and lamprophyre dykes (Lehtonen et al., 1998; Härkönen, 1994). Felsic and lamprophyre dykes possibly formed from the same magma source as the Ruoppapalo granodiorite intrusions which is located close to the Iso-Kuotko area (Härkönen, 2001 Smeds, 2015). Ore mineralization differs from the Suurikuusikko ore as gold is precipitated in fractures within arsenopyrite rather than in the crystal lattice of arsenopyrite as in the Suurikuusikko ore. Gold in the Iso-Kuotko deposit occurs as native gold within in quartz dolomite veins, which are enriched with pyrrhotite and arsenopyrite. Sayab et al. (2016) propose later deformation stage for formation of a structural jog in Iso-Kuotko which served as trap for gold precipitation. This proposal is backed up by the earlier study of Patison et al., (2007).

1.2 Orogenic gold

Temporally orogenic gold deposits are mostly concentrated in three epochs of Earth history: (1) Neoarchean 2,8 - 2,5 Ga, (2) Paleoproterozoic 2,1 - 1,8 Ga and (3) Phanerozoic 0,5 - 0,05 Ga (Goldfarb et al., 2001). Additionally, Goldfarb et al., (2001) disclose that temporal pattern is not random, but it is linked to the major supercontinent forming periods where new continental crust is formed. Orogenic gold deposits within CLB have mainly formed in the Paleoproterozoic epoch between 1,91 and 1,79 Ga (Eilu, 2015). The timing of Au-mineralization events within CLB are divided into two periods, the first was between 1,92 and 1,85 Ga and the second between 1,77 and 1.76 Ga (Molnar et al., 2018). Eilu (2012) adds that most of the deposits were formed during continent-continent collision event during the evolution of Fennoscandian shield with some exception associated with microcontinent accretion around 1,92 - 1,88 Ga.

Large-scale fluid migration occurs in supercontinent forming processes (Goldfarb et al., 2001). If sulphur-bearing fluids travel within a compound fracture network towards a major fault zone, gold can be transported within the fluids along the flow path. Gold likely enriches in secondary or tertiary fault zones, which are close by to the major fault zone, but at shallow crustal levels (Goldfarb et al., 2001). The mode of plate tectonics is not the key in orogenic gold deposits, since any hydrous and sulphur-bearing thermal event in juvenile crust, whether Precambrian plume-like event or younger collision/subduction type process, can form orogenic gold deposits (Goldfarb et al., 2001).

1.3 Aim of the study

The study area is both in geochronological and petrological sense extensively investigated (Smeds 2015, Molnar et al., 2018 and Sayab et al., 2019), but a detailed structural study has not been made. Earlier studies have used the same drill holes and field measurements, but they lack a geometrical aspect of the structural geology. This study aims to combine existing data and new observations by linking them up into bigger picture and interpreting the regional structural patterns and continuities. A key part of this study is finding structural linkage to earlier deformation phases and recognizing second and third order movements and their possible linkage to mineralized fluids, and eventually gold precipitation. This research additionally focusses on distinguishing different vein orientations and sets, and their mutual relationships. Through improved understanding of the auriferous vein systems within the Iso-Kuotko deposit mineralizations framework, forthcoming prospecting endeavours and potential mining initiatives can be strategically concentrated, and their efficacy enhanced.

2. Structural features and tectonics in orogenic gold deposits

The forming of orogenic gold deposits depends on timing of auriferous fluids in structural evolution of an orogenic belt (Groves et al., 2018). Gold carrying fluids are controlled and transported mainly by large scale crustal shear zone and faults, whereas the distribution of gold deposits is determined by second- and third order structures (Groves et al., 2000). Pre-existing structural features can be reactivated in later deformation stage when compressional stress changes to transpressional stress (Groves et al., 2018). Consequently, understanding structural geometry is key in locating orogenic gold deposits instead of accurate interpretation of deformation history (Groves et al. 2000). Repeated reactivation processes of pre-existing structures may lead to multiple mineralization stages (Groves et al., 2000). Reactivation of earlier structures occurs in Iso-Kuotko gold mineralization as reopened veins. All of the orogenic gold deposits in Finland are structurally controlled, typically occurring within 0,5- 3 km from the major first order fault zones. (Eilu, 2015),.

Common features in orogenic gold deposits consist of sub horizontal extensional quartz veins with cross-cutting acute angled fault-related veins (Sibson et al., 1988). These low- and high-angle veins form as response to a valve and pump mechanism leading to fluid pressure fluctuations (Sibson et al., 1988). Orogenic gold deposits can be found at varying depths from 3 km to 15 km (Figure 2) (Goldfarb and Groves, 2015). According to Groves et al. (2000), ductile to brittle structures with multiple types of faults e.g., strike-slip, reverse or oblique or fracture clusters are the most frequent hosting structures for gold deposits. These structures contain post- or syn mineralization displacements (Groves et al., 2000).

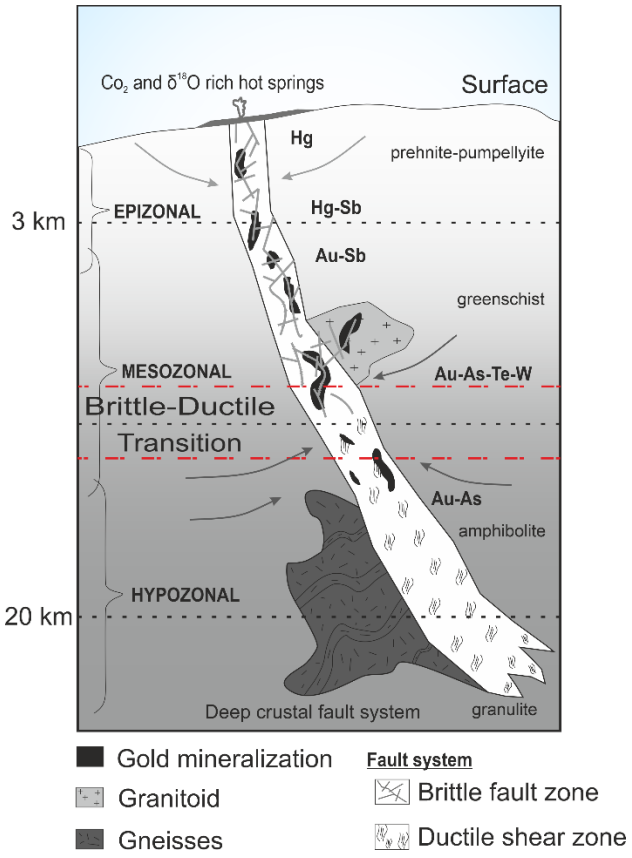

Figure 2. Orogenic gold deposits at varying depths and Au deposit associated element distribution (As, Hg, Sb, Te, W). Modified after Goldfarb and Groves, 2015.

Gold is mainly transported in low-salinity, near-neutral H_2O-$CO_2 \pm CH_4$ fluids, and is deposited as a reduced sulphur complex in the ores. These fluids linked to this type of gold deposit are characterized by their consistently high CO2 content (Groves et al., 1998). Groves et al., (2000) add that fluids also contain N_2, and gold deposits from these low-salinity fluids have characteristically high Au:Ag ratios and contain low amounts of base metals and tin.

2.1 Veins

Veins are formed in geological activities after the formation of the host rock (Bons et al., 2012). Investigations of the shape, internal structures and orientation of veins provide constraints about pressures, paleo-stress fields, and deformation kinematics (Bons et al., 2012). Most of the veins are related to fracture mechanics, since veins are mainly formed in space generated by fractures (Bons et al., 2012). Veins have diverse internal structures and textures due to variations in growth direction and crystal shape (Bons et al., 2012). There are three types of veins: syntaxial, stretching and anitaxial veins, which differ from each other by e.g., formation event, crystal growth and shape and by age distribution of precipitate (Bons et al., 2012). Anitaxial veins do not require a crack-seal event to

form, whereas syntaxial and stretching veins need at least one crack-seal event to form. Globally the two most wide-spread minerals found in veins are quartz and calcite (Bons et al., 2012).

2.2 Shear fracture development

Gold bearing veins are rarely formed by a single precipitation and transport event, but rather during several phases of deformation with associated fluid movement (Goldfarb and Groves, 2015). Fractures provide a path and a space for vein forming fluids to transport and precipitate (Bons et al., 2012), thus vein shapes are macroscopically controlled by fracture mechanisms. There are three types of fractures in brittle failure modes: extension, shear, and hybrid fractures (Bons et al., 2012). Specifically, hybrid fractures are combination of both extension and shear fractures (Figure 3).

Fractures develop in various ways with respect to brittle deformation. In strike-slip fault regimes fractures firstly develop typically as Riedel shear fractures (R-fractures), which are in a low angle to the overall shear zone (Figure 3) (Fossen, 2010). Additionally, other Riedel fractures are R' and P-shear fractures. R'- shear fractures are antithetic, meaning shear sense is opposite to the main shear and they form in high angle towards the main shear. P- shear fractures are developed mainly after R-fractures and are suggested to being formed by temporal variations in the local stress field as the shear zone deformation progresses (Fossen, 2010).

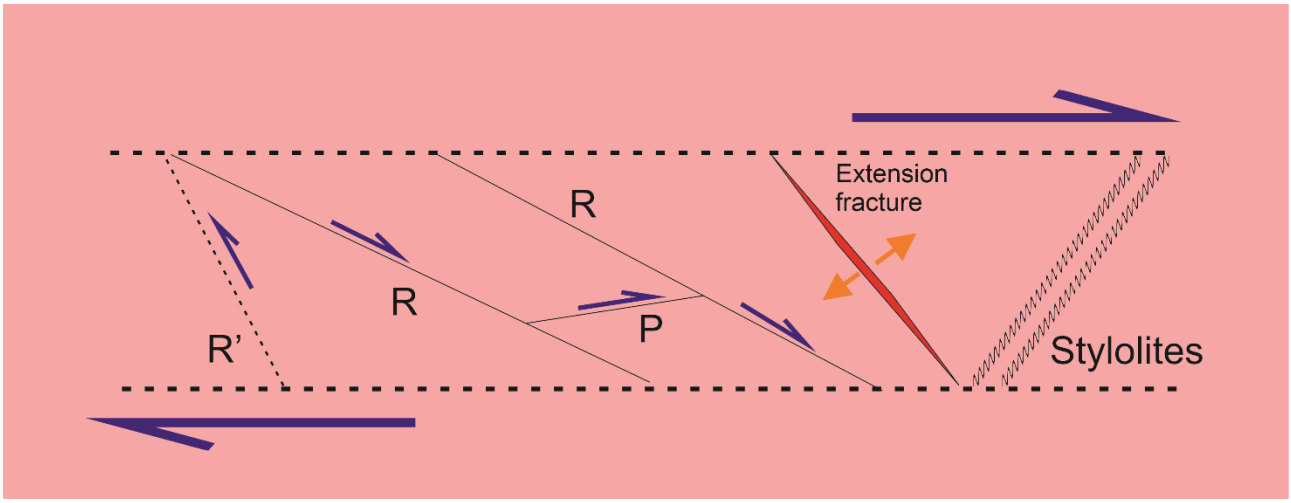

Figure 3. Dextral strike-slip shear zone and structures formed within. Riedel-model R synthetic and antithetic R' Riedels. Secondary P shears which can connect R and R' surfaces. Modified after (Fossen, 2010).

3. Regional geological setting

The Paleoproterozoic Central Lapland Belt (formerly Central Lapland Greenstone Belt/CLBG) is part of a larger greenstone belt, which extends from the Norwegian coast to the Russian Karelia (Huhma, et al. 2005). In northern Finland CLB plunges beneath southwestern contact of the Lapland granulite belt, while in the east and west CLB is surrounded by Archean granite gneiss terrains (Huhma, et al., 2005). Northwest and south of CLB are in contact with granitoid intrusions. The whole CLB is deposited over the Archean basement gneisses of the Fennoscandian shield. The CLB registers a geological evolution for over 500 Ma climaxing in orogenic deformation as a consequence pinching between the Svecofennian orogeny from south and thrusting of Lapland granulite belt from northeast around 1,9 Ga (Huhma, et al., 2005). Köykkä et al. (2019) state that CLB contains mostly 2,44 - 2,05 Ga extruded mafic to ultramafic supracrustal rocks, felsic lamprophyric/porphyritic intrusions (1,92 - 1,88 Ga) and 1,80 Ga post orogenic granitoids. Supracrustal rocks are be divided into six lithostratigraphic groups and/or suites from oldest to youngest: (1) Vuojärvi suite, (2) Salla, (3) Kuusamo, (4) Sodankylä, (5) Savukoski, (6) Kittilä (Kittilä suite) and (7) Kumpu group (Figure 4) (Lehtonen et al. 1998, (Huhma et al., 2018).

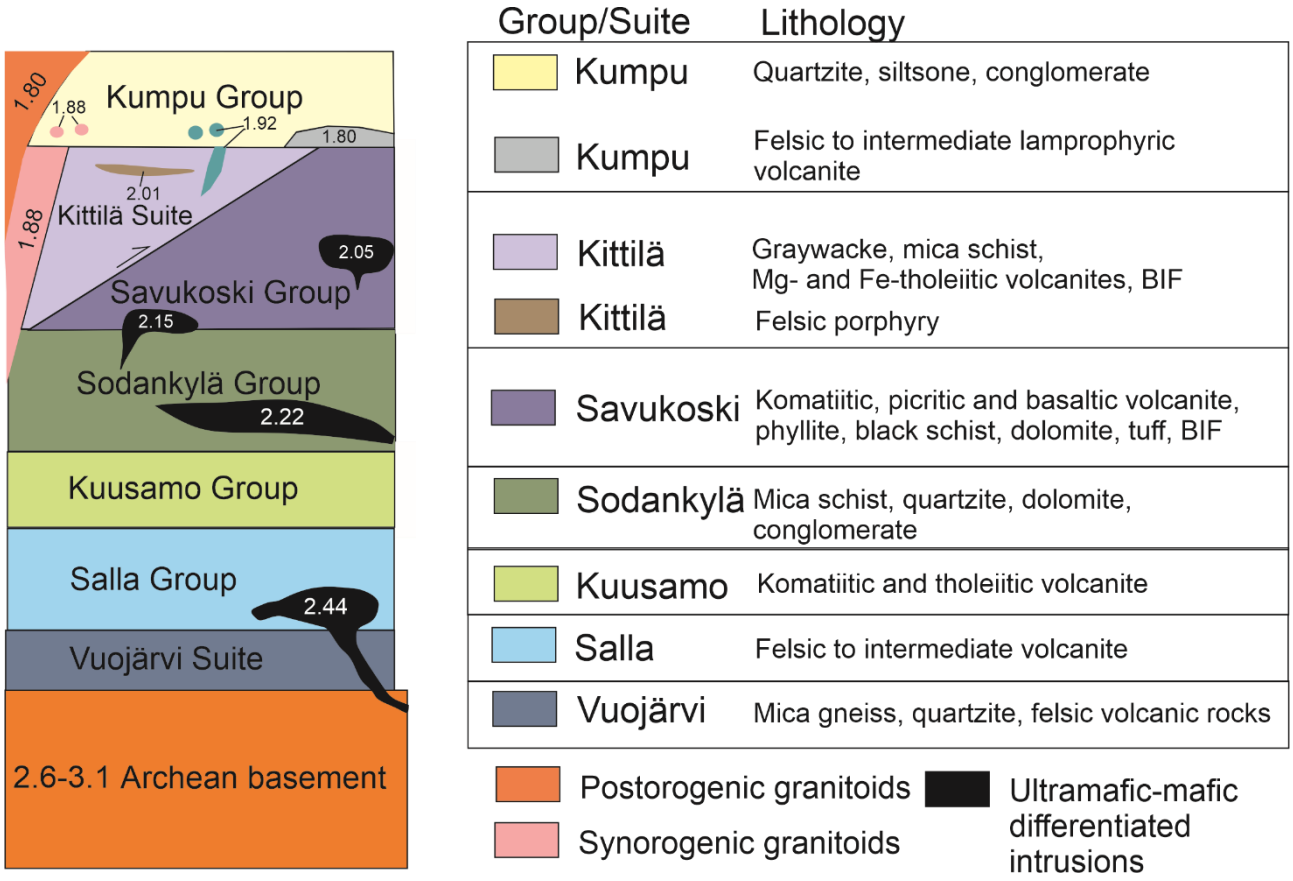

Figure 4. Lithostratigraphic and lithodemic units of Central Lapland Belt (Modified after Lehtonen et al., 1998, Huhma et al., 2018).

According to Huhma et al. (2018) the first Paleoproterozoic rocks deposited on top of Archean TTG gneisses, small greenstone belts, mica schist and granitic intrusions were Vuojärvi groups (1) quartzites, mica gneisses and felsic volcanics. The subsequent Salla group (2) rocks were deposited/emplaced on top of the Vuojärvi group. The Salla group (2) rocks are intermediate to felsic metavolcanics and some more mafic-ultramafic differentiated intrusions (Huhma et al., 2018). The Salla group was followed by Kuusamo groups (3) komatiitic and tholeiitic metavolcanic rocks around 2,44 Ga. After Kuusamo group early rift related rocks were extruded, a more stable time period followed. In this stable period the Sodankylä group (4) quartzites, mica schist, dolomites and conglomerates were deposited. These sedimentary derived rocks are cut by mafic to ultramafic sills which have been age determined around 2,2 Ga, which gives minimum age to Sodankylä groups rocks. Approximately 2,05 Ga Savukoski group (5) basaltic, picritic and komatiitic volcanics extruded along with sedimentary rocks: phyllite, dolomite, black shist, tuff, and banded iron formation (BIF) on top of Sodankylä group rocks. Around same time Kevitsa layered intrusion was emplaced (Mutanen and Huhma, 2001). A bit later 2,0 Ga marks time for events which lead to formation of the Kittilä suite (6) which is described later in detail. Lastly, topmost unit of CLB, Kumpu groups (7) characteristic felsic sedimentary rocks, felsic to intermediate volcanics were set. Also, lamprophyric dykes intruded around same time as Kumpu group rocks between 1,92 - 1,88 Ga.

3.1 Kittilä suite

While the majority of rocks within CLB are autochthonous in character, the Kittilä suite is considered to represent an oceanic allochthon (Hanski, 1997; Hanski & Huhma 2005). The Kittilä suite is enveloped by granitoids towards the south (Central Lapland Granitoid Complex), west (Haaparanta suite), and north (Hetta Complex; Rastas et al., 2001), whereas the eastern contact is against the Sodankylä group schists. The Kittilä suite is summarized by Lehtonen et al. (1998) of being bordered by faults and/or thrust contacts to the surrounding lithostratigraphic units. The Kittilä suite stands out from its' surrounding rocks as it has lower metamorphic grade than the rest (Hölttä et al., 2007). The Kittilä suite comprises of four formations: Kautoselkä, Porkonen, Vesmajärvi and Pyhäjärvi (Lehtonen et al., 1998).

3.2 Kautoselkä formation

According to Lehtonen et al., (1998) the Kautoselkä formation consists of three different distinguishable lithologies; Kaunislehto, Ikkarinvuoma and Jurpulehto members. The Kaunislehto member has massive and porphyritic lavas associated with amygdaloidal rocks, while Ikkarinvuoma member comprises mostly of sedimentogenic rocks. Lehtonen et al. (1998) add that Jurpulehto member origins from volcanic and volcanosedimentary rocks such as tuffs, graphite-sulphide schists,

mafic lavas, and conglomerates. (Hanski and Huhma, 2005) suggest Kautoselkä formations mafic lavas are Fe-tholeiitic.

3.3 Porkonen formation

The strong electromagnetic conductors within the Kittilä greenstone belt are attributed to Porkonen formations rocks (Wyche et al., 2015), which mostly comprise of mafic lavas, graphite bearing tuffs/tuffites, cherts as well as well-known banded iron formation within the CLB. Banded iron formations are further divided into carbonate-, oxide- and sulphide-facies formations.

3.4 Vesmajärvi formation

The Vesmajärvi formation consists of the other type of tholeiitic mafic lavas, Mg-tholeiitic with typical oceanic lava textures; pillow lavas and pillow breccias, hyalotuffs, agglomerates and volcanic breccias (Lehtonen et al., 1998). These volcanogenic rocks are suggested of being the youngest volcanics in the Kittilä suite. Chert, black schist, and carbonate rocks are found in Vesmajärvi formation (Lehtonen et al., 1998). Hanski and Huhma (2005) studied Mg-tholeiites further and pointed out that the Mg-tholeiites are similar geochemically to tholeiites formed in mid ocean ridges.

3.5 Pyhäjärvi formation

Pyhäjärvi formation embodies mainly quartz rich mica schists with greywacke origin (Lehtonen et al., 1998). Pyhäjärvi formation lies in the middle of synformal structure, which implies that it is the youngest formation of Kittilä lithodeme (Lehtonen et al., 1998).

4. Tectonic evolution

The study conducted by Köykkä et al. (2019) establishes a framework for the CLB, identifying five discernible tectonic stages. These stages, chronologically ordered from oldest to youngest, encompass: 1. Initial rifting, 2. Syn-rifting, 3. Syn-rift to early post-rift, 4. Passive margin, and 5. Foreland system. It is posited that the initial rifting stage could be attributed to the breakup of the supercontinent Kenorland, as discussed by Köykkä et al. (2019).

Studies conducted from CLB have quite similar timing in the main deformation stages, but the actual amount of deformation stages varies from three to five stages (D1-D5). Differences come from dividing the deformation to ductile only or both ductile and brittle deformation stages. D1 deformation is characterized by E-W shortening (Figure 5, A) caused by collision between Karelia and Norrbotten lithospheric blocks around 1.92Ga (Lahtinen et al., 2018).

D2 deformation stage (Figure 5, B) occurred between 1.90 and 1.89 and it caused N-S shortening regionally in CLB (Ward et al., 1989; Lahtinen et al., 2018). Hölttä et al., (2007) suggests that the second (D2) deformation is the most prominent structural feature seen in most of the rock types. It is seen as the main foliation S2 subparallel to bedding. D2 formed F2 folding where S2 foliation is an axial plane foliation to almost isoclinal folds which deform S0 bedding.

D3 deformation stage (Figure 5, C) took place between 1.88-1.87 and it caused formation of N and NE trending shear zones in CLB (Nironen, 2017; Lahtinen et al., 2018). Within this period tectonic setting switched from compression to transpression and caused the jog at the Iso-Kuotko gold deposit (Sayab et al., 2019).

D4 deformation stage (Figure 5, D) occurred between 1.84 and 1.83 (Nironen, 2017). This deformation stage encompasses switch in the regional stress regime from NE-SW to NW-SE (Sayab et al., 2017). This deformation also flipped the kinematics of Kiistala shear zone (KiSZ) from dextral to sinistral (Sayab et al., 2019).

D5 deformation stage (1.77 – 1.-76) (Figure 5, E) is dominated by E-W shortening, causing localized dextral shearing, veining, and fracturing at the Iso-Kuotko gold deposit (Patison, 2007). Mineralization of gold in Iso-Kuotko is proposed to take place at this deformation stage (Molnár et al., 2018).

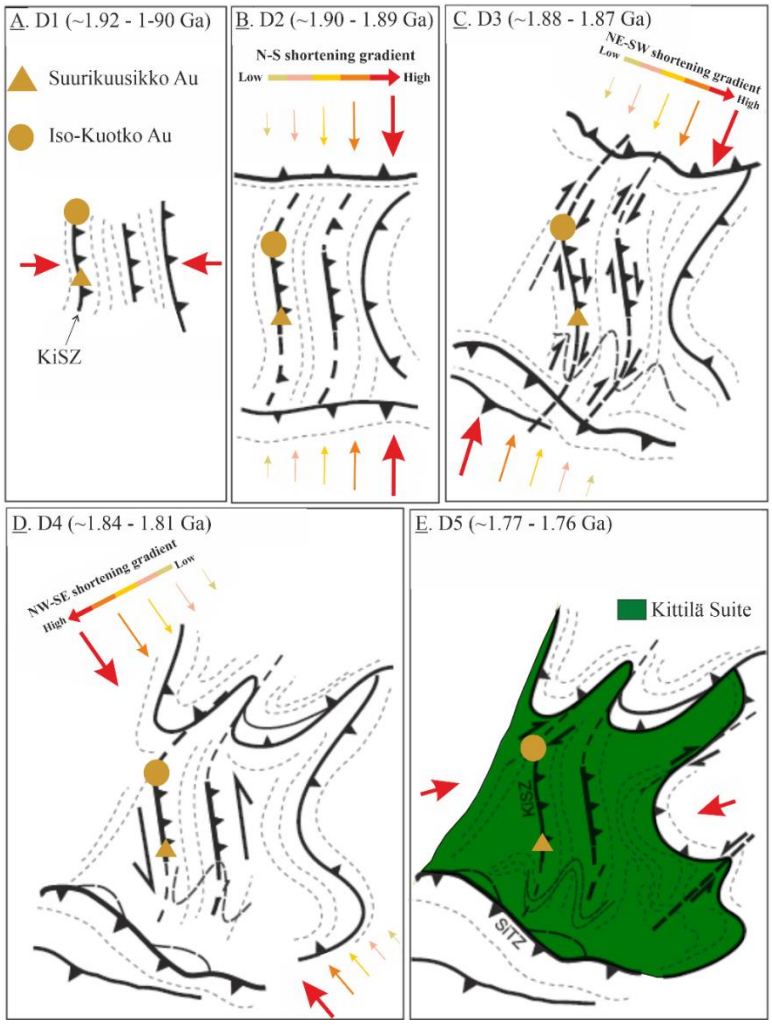

Figure 5. Deformation phases in CLB. Modified after Sayab et al., 2019.

4.1 Structures in Iso-Kuotko

Iso-Kuotko area displays several stages of shear zone development throughout its evolution (Figure 5) (Sayab et al., 2019). The most dominant deformation structure KiSZ trends approximately NE, and the smaller Kuotko shear zone (KuSZ) trends NW (Molnar et al., 2018). Niiranen (2015) attributes the KiSZ to listric thrust tectonics rather than oblique and/or steep strike-slip tectonics. With assumption of thrust related tectonics rather than steep strike-slip/oblique shear zones, Niiranen (2015) divides Kittilä terrane into four different structural domains: Kapsa-Vuotso, Seurukarkea-Kiistala, Nuttio and Sirkka-Venejoki domains (Figure 6). By contrast Molnár et al., (2018) uses the earlier model of steep shear zones as the conceptual model in their study. The KiSZ and KuSZ in Iso-Kuotko, are in close proximity to Ruoppapalo shear zone (RuSZ) and possibly linked to it by old deep structures (Niiranen, 2015). Niiranen (2015) interprets that RuSZ is initiated by collision of Kola and Karelia cratons ~1,91 Ga and thrusting of Granulite belt to SW. Sayab et al. (2019) interpret KiSZ as

a part of west-verging thrust system based of seismic data. Sayab et al. (2019) continue that steepness of KiSZ at the surface is a result of later strike-slip reactivation.

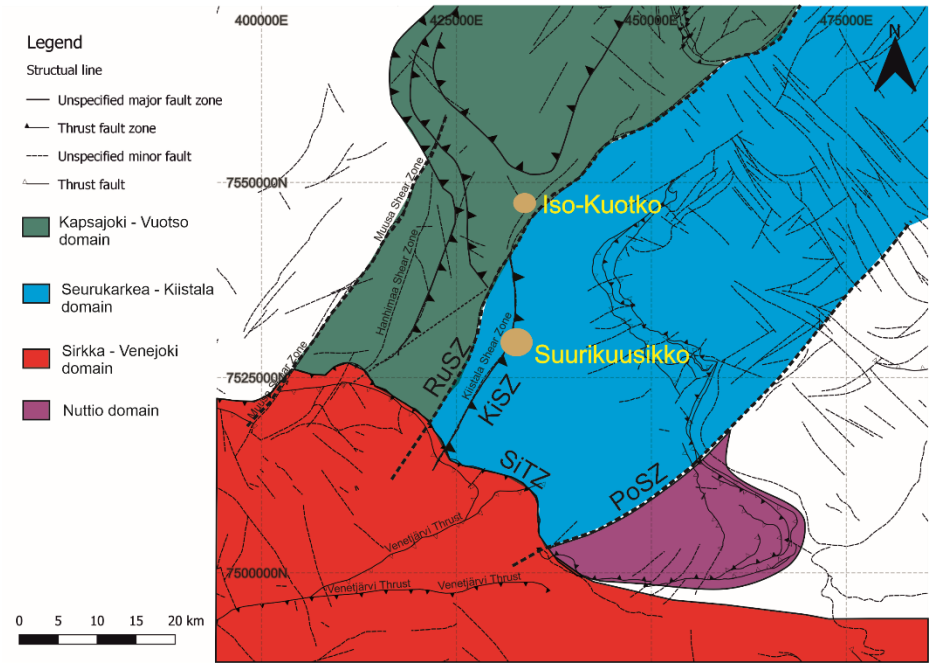

Figure 6. Kittilä terrane domains. Modified after Niiranen (2015) and GTK's structural trend line data.

Field studies from the Iso-Kuotko exploration trench (Figure 7) (Patison, 2001) reveal that there are at least three fabrics in rocks of the Kati target area. Patison (2001) notes that 'fabric' term in her study is a generic term for cleavage, compositional layering, or shear-generated foliations. The first fabric, according to Patison (2001), strikes towards NW and has moderate to steep dips. This fabric is overprinted by later fabrics thus it was difficult to observe (Patison, 2001). The next fabric as reported by Patison (2001) is crenulation cleavage with varying intensity, NW- to NNW strike and moderate to low- angle dip. The first two fabrics presented by Patison (2001) occurs mostly in the least altered rocks. The third fabric has a slaty appearance with a moderate to high-angle dip and a strike of NW. The fabric is suggested by Patison (2001) to be result of one of the three shear deformation events.

Strikes of the above shear zones are approximately towards ENE, NW, and N. Slip lineation measurements with low-angle plunge from all three shear generations imply dextral oblique strike-slip movements (Patison, 2001). Patison (2001) field studies reveal that sulphide-bearing veins are distinguishable in all three shear zones, the most abundantly in NW striking shear zone/faults. According to later study by Patison (2007) mineralized veins are synchronous with shear and they occur as shear fill in dextral strike-slip shears. Molnar et al., (2018) distinguished three types of veins with varying mineralogy, all cross cutting crenulated foliation of the host rock.

5. Methods and data

Methods for obtaining sufficient data for this study consists of large scale (10kmx10km) geophysical maps all the way to millimetre scale drill core structure measurements. Data interpreted from broad scale features such as foliations, shear zones and folding are combined with regional scale fractures, faults and lineations for describing study area geometry and structural continuity. The aforementioned structural features are visualized separately and as combined with 3D modelling and lower hemisphere projections.

5.1 Regional structural analysis

Regional structural analysis is based on Geological Survey of Finland (GTK) geophysical low altitude flight data gathered between 1973 and 2007. Geophysical magnetic anomaly data in this study is used for interpreting large scale structural trends such as foliations, folds, and shear zones. Structures are drawn as trend lines across the mapped area. Trend lines are further used as a reference for smaller scale structural work, and they are confirmed and compared with more precise field observations and drill hole investigations. Dips and dip directions of the trend lines are lacking in the Figure 10, due to absence of structural measurements from the area available for this study.

5.2 Field observations

Although there is abundantly previously collected field observations, the data was still lacking with detailed smaller scale measurements as most of the previously collected data was targeted for finding mineralized veins and shear features. Especially shear related veins had been in primary focus as they are commonly gold bearing, according to earlier studies by Molnar, et al., (2018); Smeds, (2015); Patison, (2007).

M1ISO2020 (Figure 11) trench is located in the ‘Retu’ gold mineralization target of Iso-Kuotko area. A detailed lithological mapping is not made due to weathering of the trench and early snowfall in autumn 2021. MSc Kåre Höglund constructed a detailed lithological map of the trench in 2009 when it was excavated. In this study two trenches were investigated structurally with prof. Pietari Skyttä in the study area. 26 structural measurements were taken in total, from which all but one, were a planar feature. The other trench located in Tiira gold mineralization, but due to lack of measurements it is not used in this study.

5.3 Drill hole investigations

Structural geometry of the study area is based on drill core logging and measurements taken from exploration trenches. Historical drill core structural measurements are used for obtaining more precise

geometrical model of ductile features. Study area is divided into three areas related to the known mineralizations: Kati, Retu and Tiira. Drill cores from Tiira area are rubble core, therefore they could not be effectively used in geometry interpretations.

5.3.1 Drill core logging

Obtaining representative structure data for stereographic analysis from drill holes, depends on two variables: 1. Structural sets intersect drill hole axis close to 90°, and 2. Spacing between structural sets equals true spacing (Kramer Bernhard et al., 2020). Kramer Bernhard et al., (2020) adds that structure sets subparallel to drill hole axis are sampled less frequently, therefore they are marginalized in the data set. Area with only one direction of drilling may be missing an unknown structural set because it is scarcely sampled. This bias can be removed by adding at least three differently orientated drill holes (Kramer Bernhard et al., 2020).

The structural data measurements from selected drill cores are obtained with Relfex IQ-Logger device. The structures subject to observation were fractures, different type of veins, shear features, foliations and lineations e.g., slickenlines and fibres. In total 1235 structural measurements are taken from 12 drill cores. The selected 12 drill cores chosen for this study are focused around the known three gold targets around the Iso-Kuotko area, focusing mainly on the Kati target (Figure 7). Drill cores taken from the southernmost mineralization Tiira had high amounts of core loss and rubble core, thus that target could not be as thoroughly studied by drill core method as the other two targets Kati and Retu. The true amount of each vein type in each target cannot be compared with each other, since measured drill core metres are higher on Kati area than Retu area.

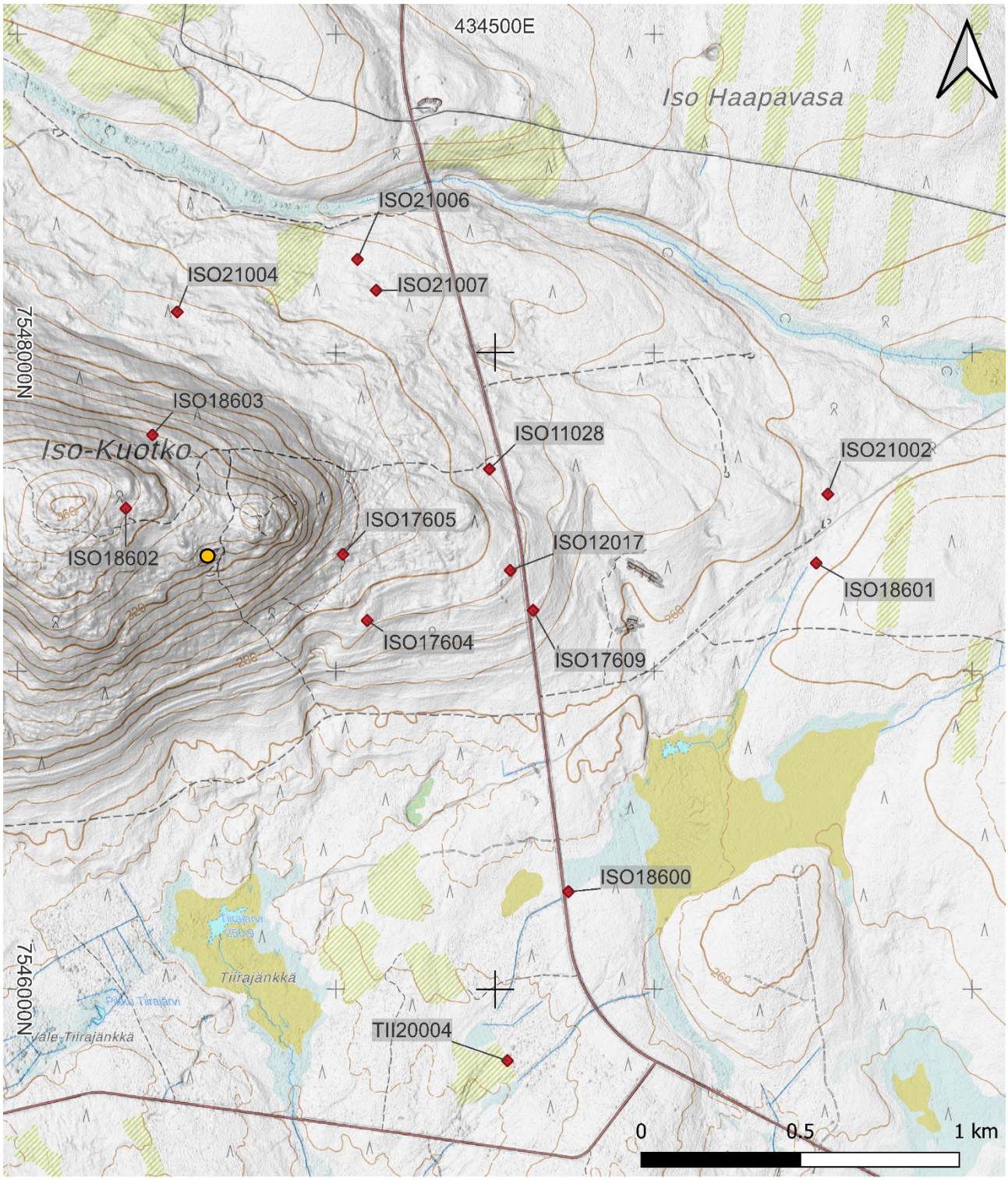

Figure 7. Drill cores used in this styudy from Iso-Kuotko gold deposit. Yellow dot = Exploration trench used in Patison (2001).

Structural measurements are focused on drill core sections which were already oriented or could be oriented for this study. A vast sections of drill core were already cut in half as they were sent to chemical analysis. Therefore, the measured meters from the drill cores are relatively short compared to the whole drill core length (Table 1). Also, vein density graphs made from drill core measurements

do not display the true amount of veins per meter, due to lack of drill core orientation. The vein density graph comprised from visually counted veins from core box images (Appendices) display more accurately veins per meter than the graphs comprised from drill core measurements (Table 1). Many drill core intervals, which contained gold bearing veins could not be measured, since they were mainly sent to analysis, and did not have orientation line anymore. Vein density graphs from drill core box images are displayed in as appendices. Drill cores ISO18600, ISO21002, ISO21007 and TII20004 are left out of results due to low amount of structure measurements.

Table 1. Logged drill cores, structural measurements, and optical imaging. *Drill core was not oriented and/or could not be oriented.

Hole ID	Measured meters	Core box image logged meters*	Measurements #	Optical imaging
ISO17604	34	206	127	
ISO17605	31	229	63(core)+308(optical)	X
ISO17609	37	223	125	
ISO18600	3	247	10	
ISO18601	15	311	78	
ISO18602	82	181	362	
ISO18603	48	224	194	
ISO21002	26	124	76	
ISO21004	70	81	104	
ISO21006	23	128	58	
ISO21007	3	154	13	
TII20004	10	140	26	
ISO11028			209	X
ISO12017			470	X
Sum	**348**	**2042**	**2223**	

5.3.2 Optical bore hole imaging

Optical bore hole imaging (OBI/OTV) offers detailed, uninterrupted, and well-oriented panoramic record of the borehole wall. These images enable the determination of the characteristics, associations, and orientations of lithological and structural planar elements. OBI is a surveying method where a camera is slowly lowered into a drill hole, and it can be done for either a dry or a water-filled bore hole. The camera records the hole and after that the video is postprocessed and split in half which enables interpretation of structures in the hole (Figure 8). This method is efficient for

holes which have had poor core recovery or are old drill cores lacking structural measurements. The quality of OBI images is influenced by various factors including drilling mud, chemical precipitates, bacterial production, and other conditions that can either cloud the borehole water or result in deposits on the borehole wall (Figure 9).

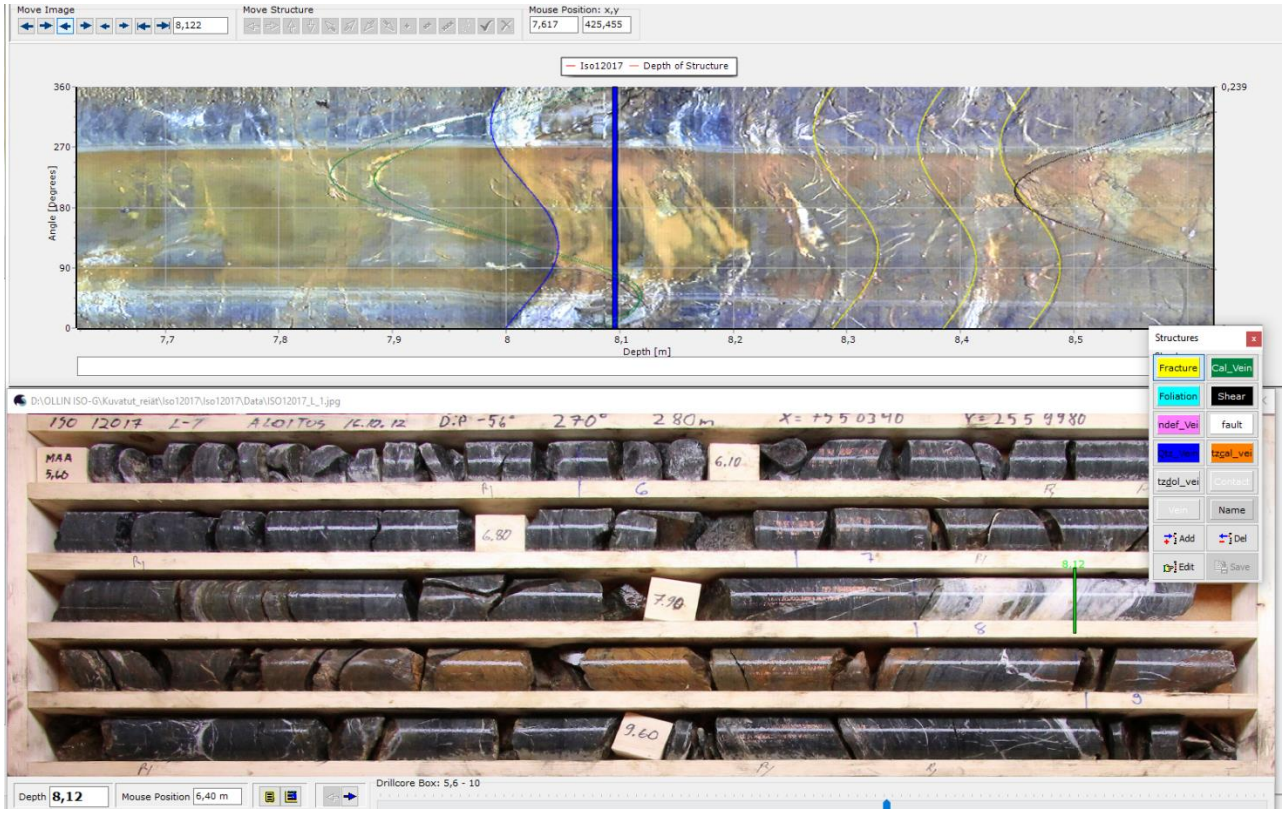

Figure 8. OBI of bore hole ISO12017 at 8,12-meter depth. Top half displays image of the video, which has been split in half. Bottom half is image of a core box at the same depth. Green line in core box displays place of the video on top half.

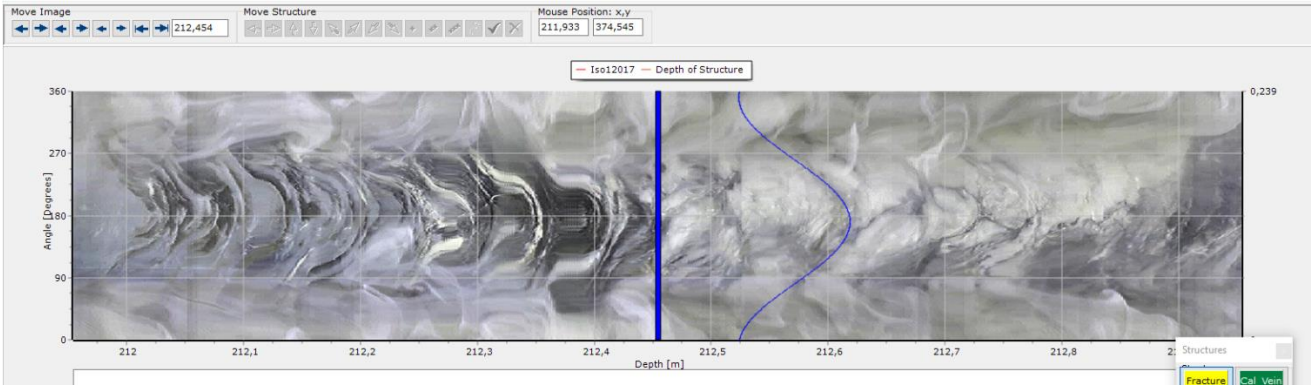

Figure 9. OBI of bore hole ISO12017 at 212,45-meter depth which has been split in half. Video is smudged due to dirt in the bore hole water.

Three drill holes are chosen for optical imaging which was done by Astrock Oy. Two of these drill holes (ISO11028 and ISO12017) are older than drill cores used for structural logging in this study. These drill holes are located in the middle of study area that lacked sufficient drill core measurements.

ISO17605 drill hole is both optically imaged, and drill core is structurally measured for comparing the two methods in reliability and similarity in results. These three optically imaged bore holes generated a total of 987 structural measurements.

6. Results

6.1 Regional structural signatures

Trend line interpretation of the regional-scale structures displays dominantly NE trends, with regional-scale open folding (Figure 10). The area illustrated in Figure 10 involves variably trending fold axial surfaces within the proximity of the E-W trending Sirkka thrust zone. Fold within the southern part of the Sirkka thrust zone area associated with E-W trending fold axis, whereas in the northern part the fold axial traces trend in more N-S direction (Figure 10). The area of this study is located at a junction of three distinct structural trends: NE-SW, NW-SE, and NNE-SSW. In vicinity of the study area the fold axial traces are trending NW-SE. The southern part of the study area is dominated by NNE-SSW structural trends (Figure 10).

Four NNE-SSW trending deformation zones are presented within the conducted regional scale geophysical interpretation: Muusa, Hanhimaa, Kapsajoki and Kiistala deformation zones (Figure 10). All these zones abut against or are adjacent to the Sirkka thrust zone. Deformation zones are linear and have a characteristically negative magnetic anomaly, which allows their distinction from the surrounding areas of positive magnetic anomalies (Figure 10). Deformation zones primarily intersect folds, while also, following the overall trend of the regional foliation (Figure 10). The study area is located within a bend of the Kiistala shear zone, where it changes trend from NNE-SSW to NE-SW (Figure 10).

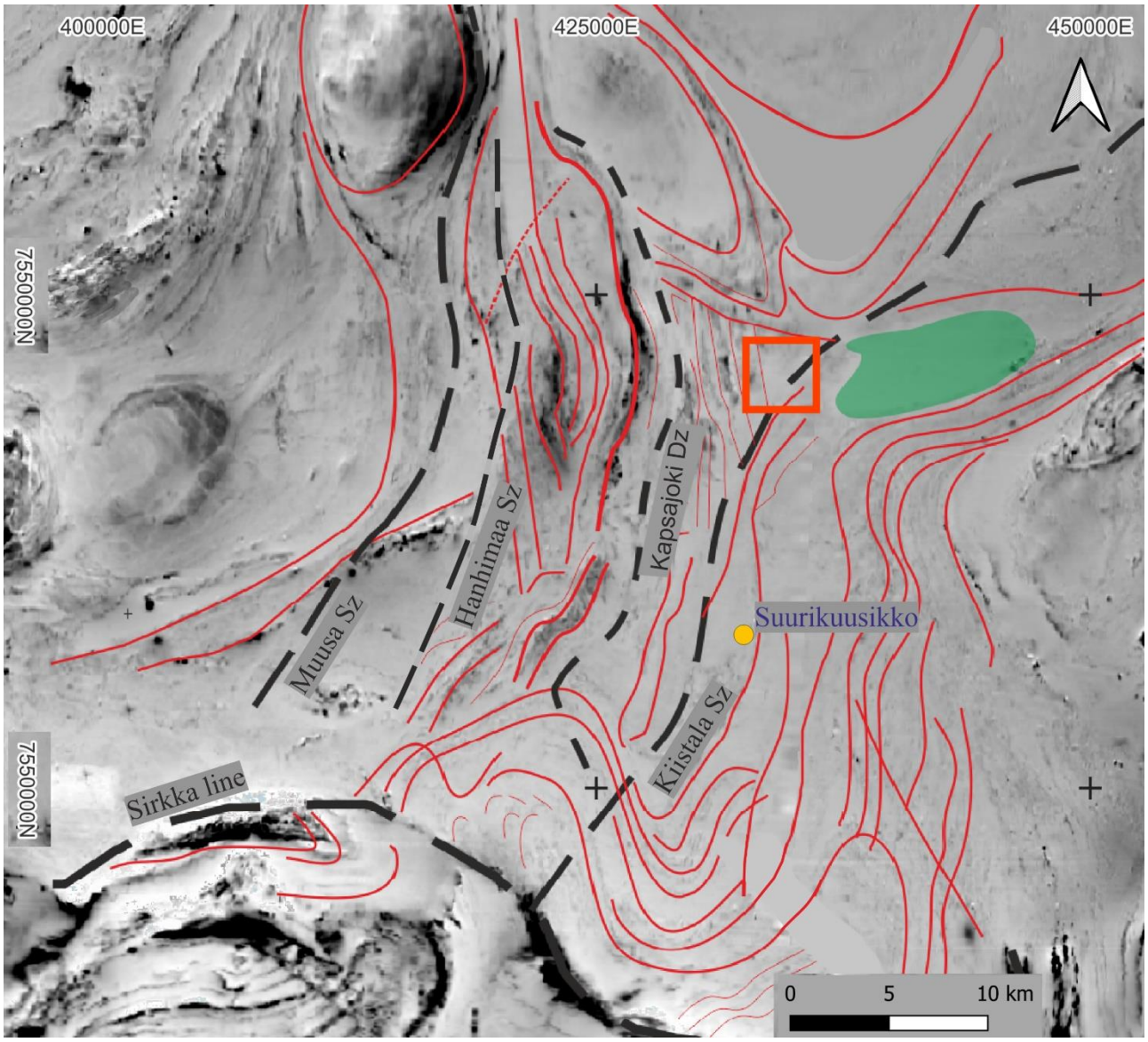

Figure 10. Regional structural trend lines interpreted from geophysical magnetic anomaly image (GTK) and(Niiranen, 2015). Orange square = study area, green area = Ruoppapalo felsic intrusion.

6.2 Field observations from an investigation trench

Characteristic rocks within the investigation trench M1ISO2020 are gently NW-NE dipping foliated mafic volcanic rocks (Figure 11, A, Figure 12, B, C). Foliation within the SE end of the trench is undulating around small-scale sub horizontal anticline whaleback folds (Figure 12, A). In the middle part of the trench, foliation of the mafic volcanic rocks becomes steeper (Figure 11, A, C; Figure 12, E) within the spatial vicinity of a subvertical NE trending fault zone (Figure 12F). This fault zone causes the development of an S-C structure indicative of a sinistral shear on horizontal level within the mafic volcanic rocks in the NW side of the trench (Figure 12, G). Additionally, in the middle part of the trench, foliation attitude changes from NW to NE.

Within the NW part of the trench, foliation steepens within the proximity of an approximately NE trending shear band. Also, a minor sinistral fault trending ~NE was measured (Figure 12, F) and a sinistral S-C structure (Figure 12, G) was observed on the western side of the shear band.

The observed quartz-carbonate veins from the research trench are situated in the central part of the excavation, near the vicinity of the sub-vertical foliation. The veins are thin, less than 3 cm wide, subvertical in orientation, and they intersect the foliation, one dipping to the east and the other to the NW. The strike of the veins closely follows the orientation of the host-rock foliation (Figure 12, D).

Both the statistical fold axis calculated from foliation measurements (Figure 11, B) and one measured fold axis (Figure 12, A) are approximately the same.

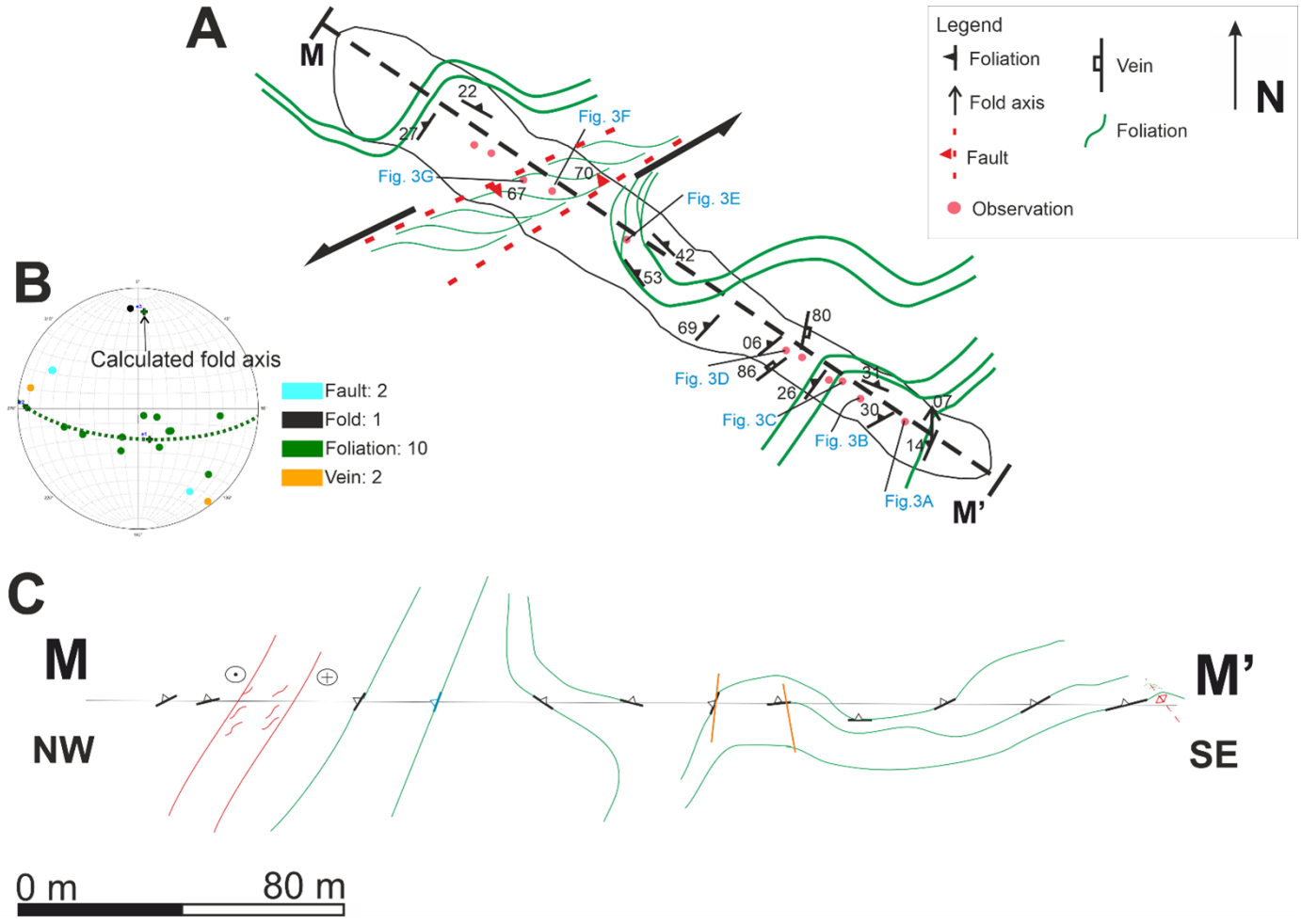

Figure 11. A. Schematic map of M1ISO2020 trench with field measurements. B. Lower-hemisphere stereographic projection of the measured structural features. The calculated fold axis is marked in the projection. C. Cross-section of the trench, arrow tips indicating sinistral movement.

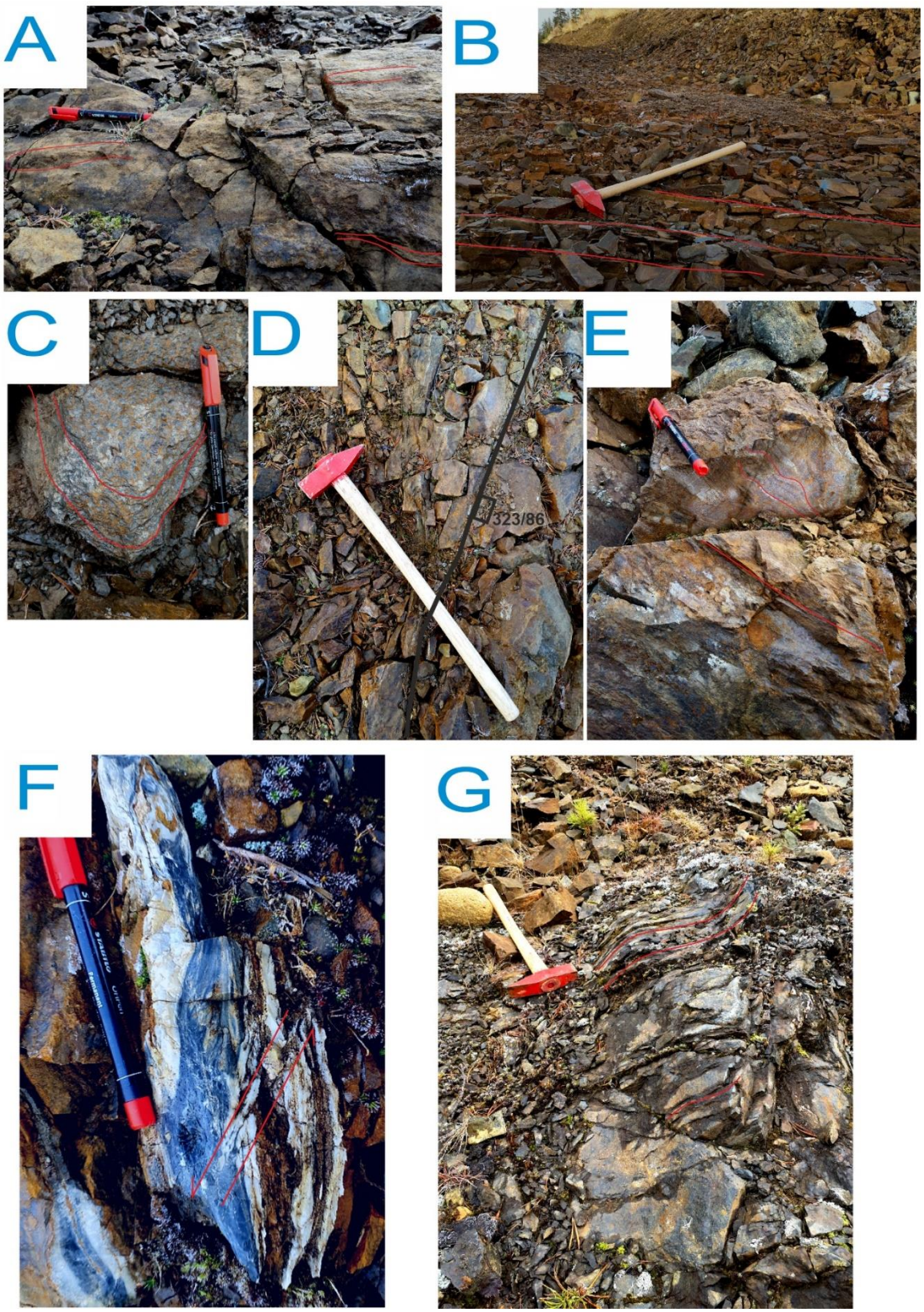

Figure 12. Field photographs from trench M1ISO2020. (A) Mafic volcanic rock with subhorizontal whale back folds at SE end of trench. (B) Subhorizontal bedding parallel foliation of mafic volcanic rock. (C) Subhorizontal foliation of chlorite schist. (D) Mafic volcanic rock cross cut by subvertical quartz carbonate vein. (E) NE dipping foliation of albite altered mafic volcanic rock. (F) Foliated carbonate rock with later sinistral microfault. (G) visual sinsitral SC structure of mafic volcanic rock. Rockhammers' (70cm) handle pointing North. Marker (15 cm) tip pointing North.

6.3 Structural geometry of the study area (based on drill hole data)

Ductile structural features, such as foliation, folding and shear bands and zones, are most visible in mafic volcanic rocks. Brittle structural features, including brittle shear zones, faults and fractures are observed in altered mafic volcanic rocks and felsic dykes. Most of the observations are from foliated mafic volcanic rocks. The more thoroughly investigated study area is divided into Kati and Retu targets, which vary in dip direction and the trend of both ductile and brittle structures.

6.3.1 Kati

The Kati area is characterized by gently (< 40°) North, NE, and East dipping main foliation (Figure 13, A). The fluctuation in dominant dip direction indicates a likelihood of open cylindrical antiform plunging moderately towards NE. Despite the fact that the foliation data displays an abundance of scatter, the poles indicate a fold axis in 030/52. Foliation steepens towards SE and turns gentle again at the edge of the modelled form surface in NE (Figure 13, A). Steeply dipping foliation in SE is likely due to the proximity of a shear zone or a shear band (Figure 13, A).

Occurrences of atypical, steeply-dipping to sub-vertical foliation planes display NNE and NNW trends (Figure 13, B), which likely indicate the presence of shear bands or other features of higher ductile strain. Scattered poles in North and Southeast in the lower-hemisphere projection display small-scale shear bands (Figure 13, B, Figure 18, Figure 22, A, B, C).

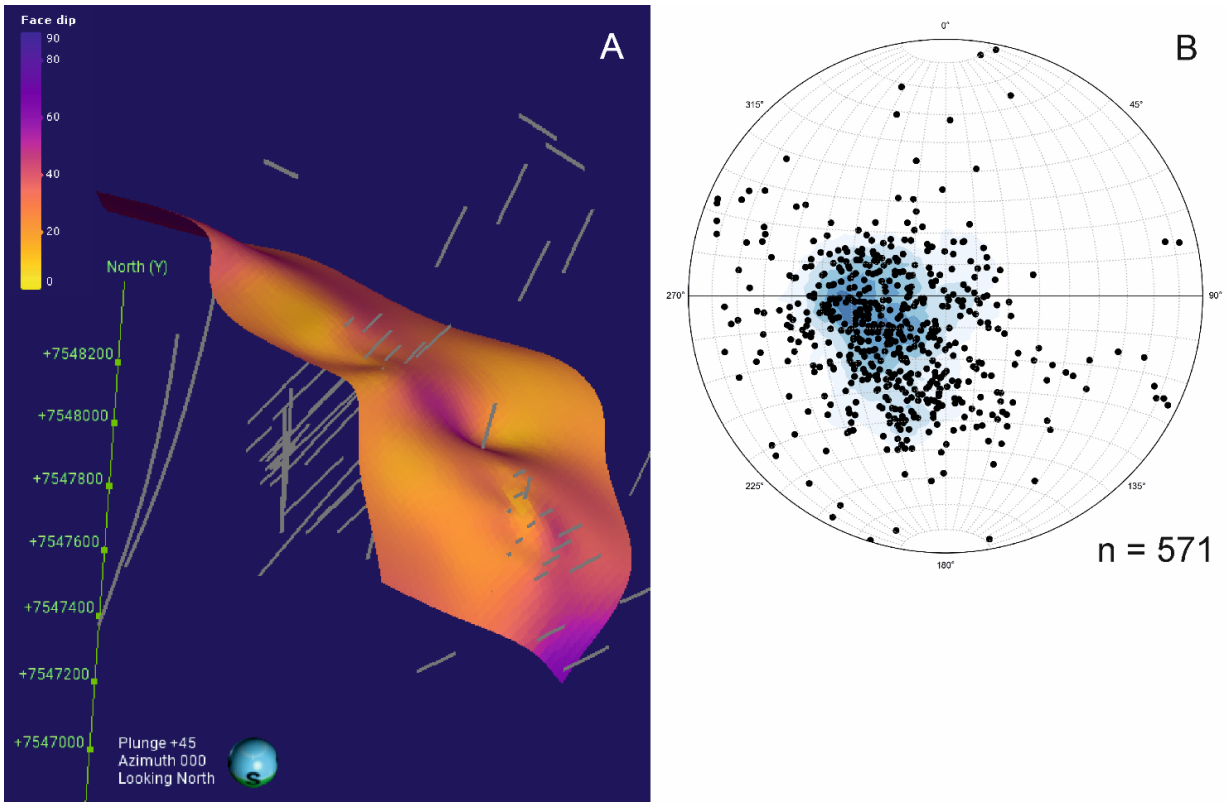

Figure 13. A. Ductile geometry of Kati area (orange to purple plane). Grey traces = drill holes used in interpolating the structural form line. View towards North at a 45-degree angle. B. Lower-hemisphere projection of the ductile measurements used in formatting the structure form surface.

6.3.2 Retu

Bedding of the mafic volcanic rocks in the Retu area is dominantly sub-horizontal and foliation is mostly following the bedding orientation. Foliation is mainly undulating from NW to SE around a gently NE plunging antiform fold. The sub-vertical NE trending Kiistala shear zone (KiSZ) causes the deflection of the foliation into a sub-vertical orientation within the Southern part of the modelled form surface (Figure 14, A). The northern part of the Retu area displays dip towards N-NW with slight variation within the overall gentle dip angle. The structural measurements display two subvertical shear measurements trending towards NE (Figure 14, B).

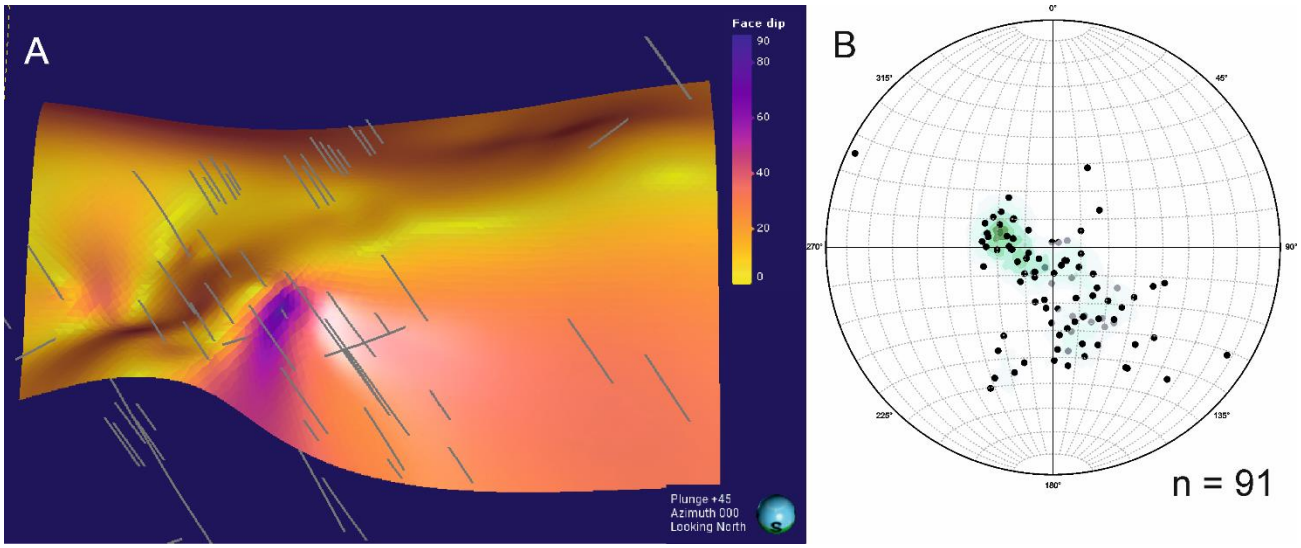

Figure 14. A. Ductile geometry of Retu area (orange to purple plane). Grey traces = drill holes used in interpolating the structural form lines. View towards North at a 45-degree angle. B. Lower-hemisphere projection of the ductile measurements used in formatting the structure form surface.

6.3.3 Shear features

In both targets, Kati and Retu, there are shear elements that are sub-parallel to the prevailing foliation (Figure 15, blue planes, Figure 16). Foliation parallel shear feature in Kati is caused by NE dipping ductile thrust fault sequence (Figure 15, blue plane). Foliation parallel, low- to moderate dipping, shear elements/crenulation cleavages are the most apparent in the least altered rocks. Gently undulating shear zone in Retu is dipping to NW with a similar undulation as shown by the surrounding foliation (Figure 15, blue plane). Shear bands are the easiest to identify from sheared veins, since they stand out from the surrounding host-rocks (Figure 16, Figure 18).

Figure 15 (red planes, Figure 17) illustrates localized subvertical shear features. In Kati, the subvertical shear bands trend towards NW and NE. In the NE part of the area, where the ductile geometry's trend turns towards NW, a foliation parallel subvertical shear band is observed. The NW part of Kati displays a NE trending shear band which cross-cuts the surrounding NW dipping foliation and foliation parallel gently-dipping shear band. Also, middle parts of Kati a NNW and a WNW trending shear bands cross-cut surrounding ductile structures.

The Retu target encompasses a local ~80 ° dipping shear band trending NE (Figure 15, red plane). The shear band is cross-cutting the surrounding foliation and causes a deflection of the host-rock foliation into steeper dips.

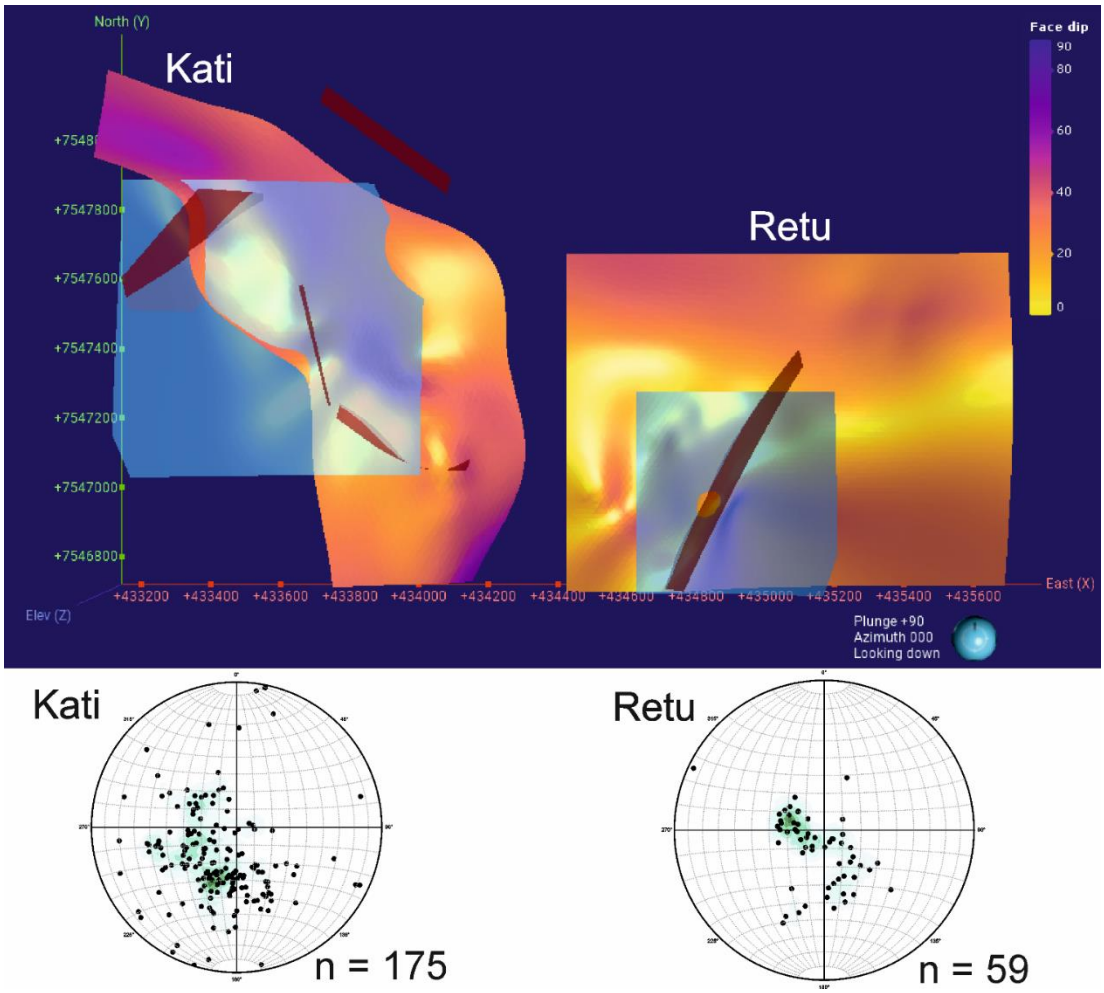

Figure 15. Ductile features plotted with subvertical (red planes) shear bands and gently-dipping (blue planes) shear zones. Gently-dipping shear feature in Kati target is dipping in same direction as the main foliation (NE). Gently-dipping shear band in Retu is dipping towards NW. Lower hemisphere projections display the shear measurements. Map is displayed straight down, north up.

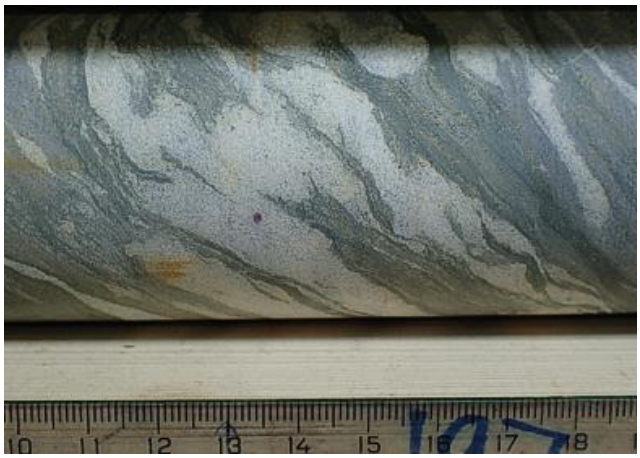

Figure 16. Drill core ISO17609 (Kati area) with foliation parallel shearing of calcite (type 4) vein and mafic tuff. Drill core was not oriented.

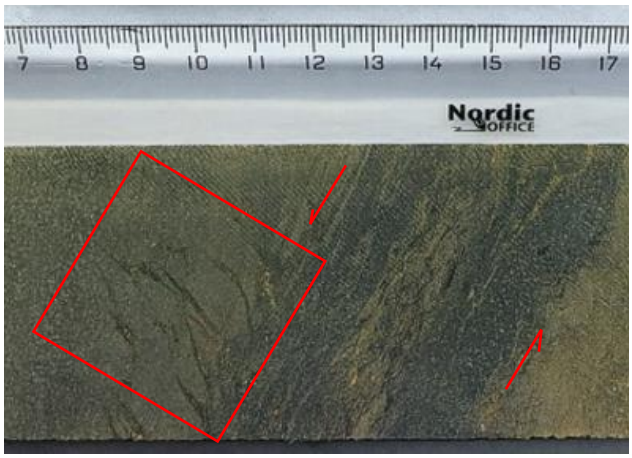

Figure 17. Drill core ISO18602 (Kati area): Sub-vertical sinistral shear band of altered mafic volcanic rock. Shearing initiated tension fractures (red square). Drill core was not oriented.

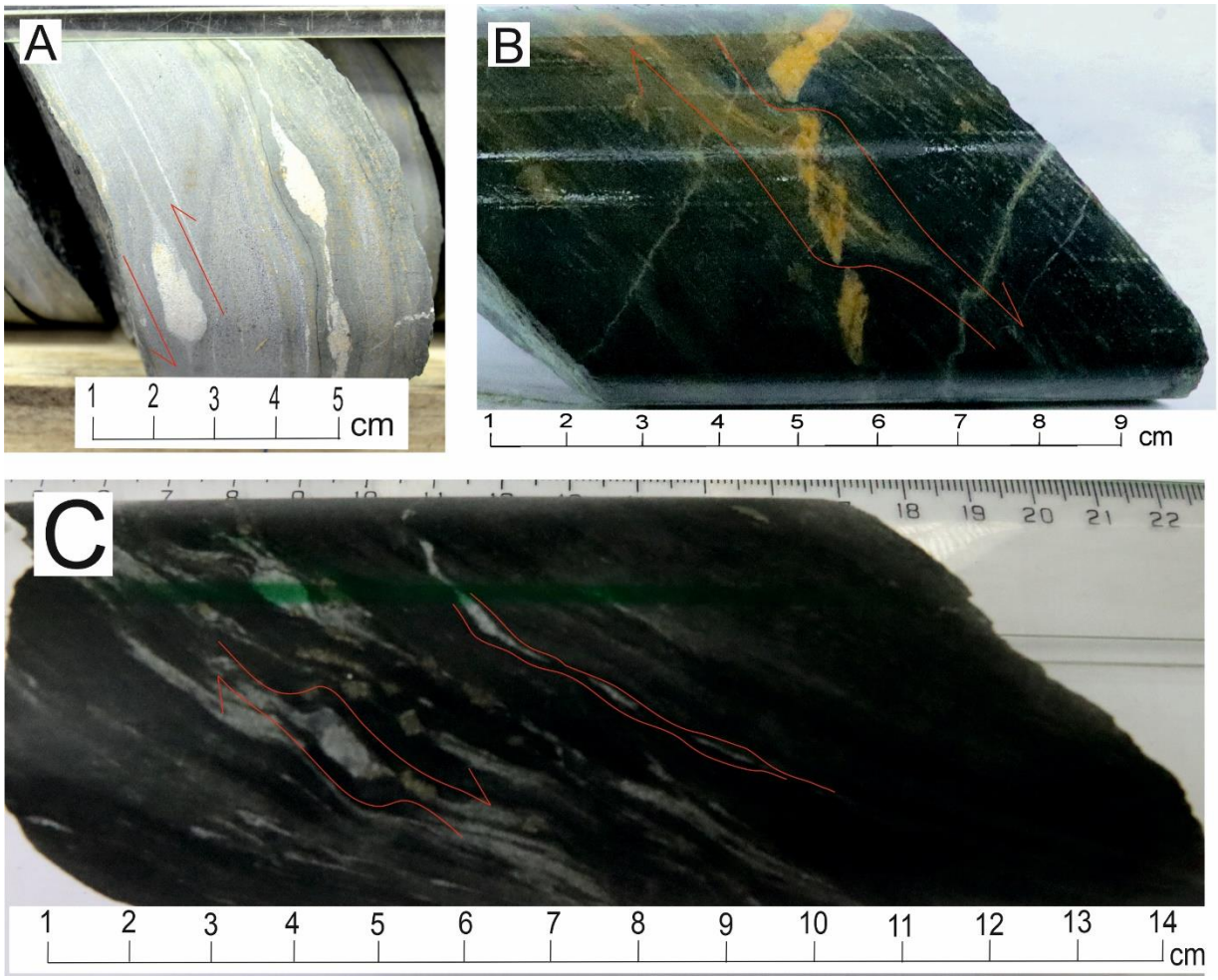

Figure 18. Shear bands. A. Drill core ISO1709 (Kati area) Extension of elongated quartz + calcite (type 5) vein along shear band. B. Drill core ISO17604 (Kati area) combination of dextral shearing along shear fractures of quartz + Fe-carbonate + sulphide (type 3) vein. Vein 012/82, shear band 100/25. C. Drill core ISO21006, NW of Kati area, dextral shearing (340/40) of sigmoidal quartz clast in mafic tuff and boudinages of calcite vein (type 4 vein).

6.4 Veins

6.4.1 Vein types

Five types of veins were distinguished from the drill cores based on their mineralogical variations (Table 2; Figure 21A-E). All five vein types occur throughout the drill cores, although usually as groups of one or two vein types (Figure 19). Veins cross-cut mafic volcanic rocks, altered mafic volcanic rocks and felsic dykes (Figure 19), except at one location, where the vein is parallel to the main foliation. All but one vein type include quartz within the mineral assemblage (Figure 21, D).

Table 2. Observed vein types and their mineralogy, gold bearing properties, cross-cutting features, and spatial occurrence within the study area.

Vein type	Mineral composition	Gold bearing(Y/N)	Cross-cuts vein types	Occurrence
1	Quartz	N	2, 3 & 4	Kati
2	Quartz + Fe-carbonate	Y	1, 3, 4 & 5	Kati & Retu
3	Quartz + Fe-carbonate + sulphide	Y	1, 2, 4 & 5	Kati & Retu
4	Calcite	N	5	Kati & Retu
5	Quartz + calcite	N	1, 2 & 3	Kati & Retu

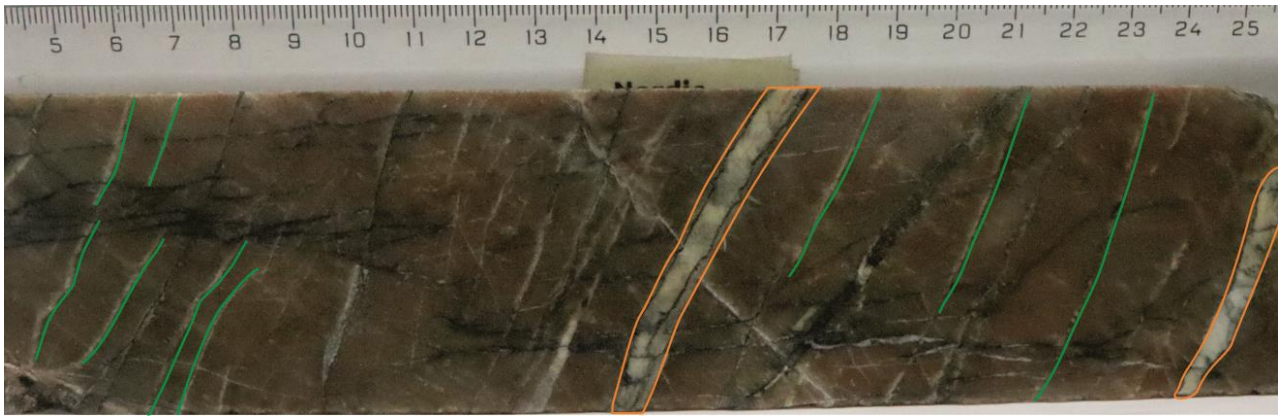

Figure 19. Drill core 18601 (Retu target). Felsic dykes of type 1 (green traces, 1mm wide) and 5 (orange traces, 3-4 mm wide) veins. Picture displays also several 1-2 mm wide magnetite filled drill core parallel fractures (black traces).

Vein type 1 displays a pure quartz composition (Table 2, Figure 21, A). Additionally, magnetite was observed in two veins. Also, in five veins, sulphides were observed in fractures and/or contacts. Quartz veins are observed to form as parallel and as cross-cutting to the host rocks. Type 1 veins are observed only in Kati area. Quartz veins vary between 1 mm and 255 mm in width, and their mean width is 27 mm. The widest quartz veins are 220 and 255 mm in width, have most likely been reactivated as they contain vein type 2 and 3 within. In drill cores where type 1, 2 and 3 coexist in close vicinity, type 1 veins have been cross-cut by type 2 and 3 veins. Quartz veins are mainly planar, but observations revealed that 5 out of the observed 44 veins had undulating texture and lineated

crystal forms. Undulation and lineated crystals confirm that some of the quartz veins have been subjected to ductile deformation processes.

Vein types 2 and 3 are both associated with gold precipitation, and both contain quartz and Fe-carbonate, mostly dolomite (Table 2, Figure 21, B, Figure 21, C). Additionally, vein type 3 includes sulphides (Table 2), primarily pyrrhotite and pyrite, and in some cases arsenopyrite. These gold bearing veins are most abundant in albite + sericite altered mafic volcanic rocks as well as in felsic dykes. Vein type 2 and 3 were observed in proximity of each other in the drill cores. Type 2 veins were 1 to 95 mm wide, with an average width of 5 mm. Quartz + Fe-carbonate veins typically cross-cut the main foliation and ductile shear bands, and they were occasionally parallel to the foliation. In five instances they were offset by shear bands, twice by faults, once by type 3 vein. 61 of 254 type 2 veins were undulating, from which 9 displayed a lineated crystal form caused by shear strain (Figure 20). The rest 193 veins were planar, from which 6 were observed with shear generated lineated crystal form.

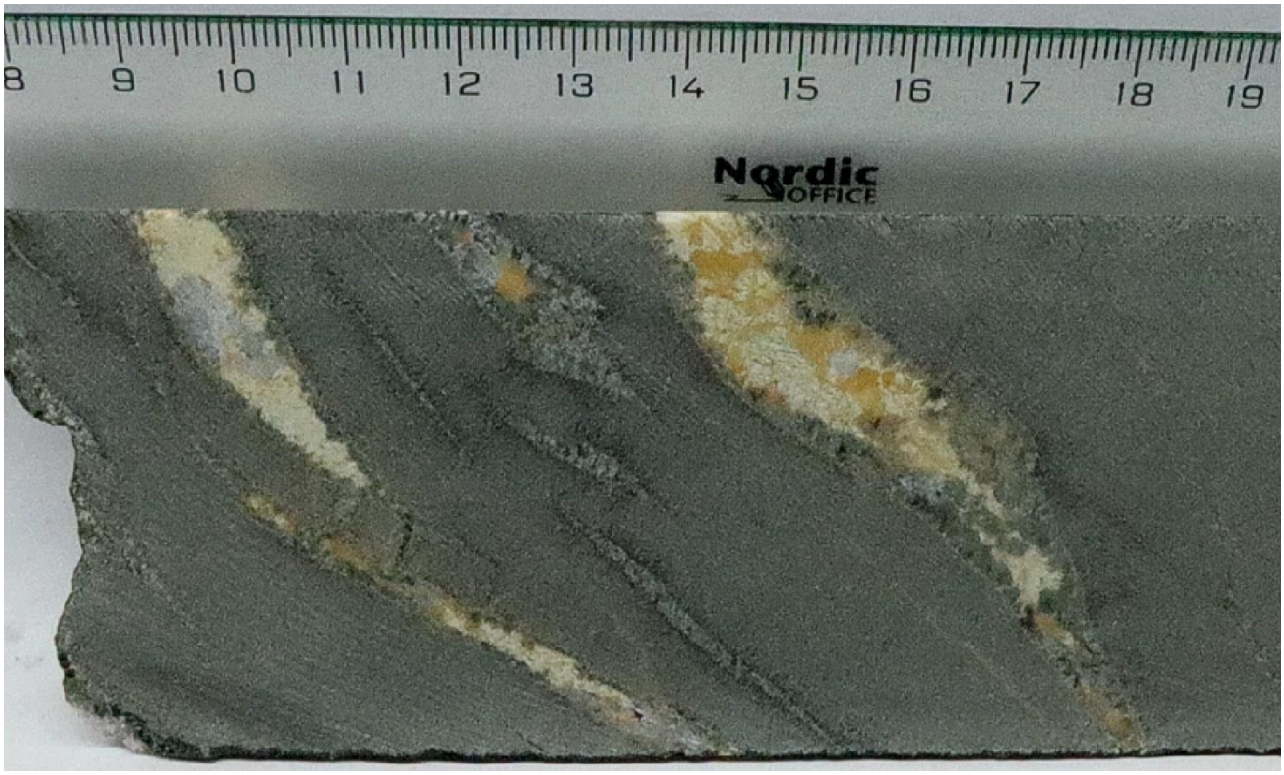

Figure 20. Drill core ISO18601 (Retu target) with sheared and boudinaged sigmoidal type 2 vein with alteration halo. Drill core section was not oriented.

The observed type 3 veins were 1 mm to 80 mm wide, with a mean width of 8 mm. Semi massive sulphide occurrences were observed within the wider ends of the veins. Sulphides were precipitated as disseminated through the vein, in contact with the host rock and the vein, and as grain clusters within the vein (Figure 21, C), or as fracture filling of quartz and/or Fe-dolomite crystals. Out of 144

type 3 vein measurements, 24 were sheared and 10 of the sheared veins were planar while the rest were undulating. Sulphide-bearing veins were observed in five occasions to be boudinaged by later shears and/or faults. Type 3 veins did not display abundance of offset by other vein types, only in one observation type 3 vein was cross-cut by type 1 vein.

Type 4 veins were solely thin, 1-3 mm wide, calcite bearing veins (Figure 21, D), which were aligned parallel to the foliation more than the other vein types, and mainly cross-cut by other vein types. Calcite veins were observed in dense intervals, but they do not have correlation with gold bearing veins. Out of 196 type 4 vein measurements, 44 veins were observed as undulated and 23 as sheared. 2 of the sheared veins had shearing parallel normal faults (~60 degrees dip angle) with calcite filling. Compared to the other vein types, calcite veins had a relative abundance of chlorite alteration haloes and disseminated fine grained magnetite minerals.

Vein type 5 comprises of quartz and calcite, where calcite appeared at the contact of the vein and the host rock, but also within the quartz fractures as well (Figure 21, E). The width of quartz + calcite veins varied from 2 mm to 120, with an average width of 7 mm. 17 of 145 veins displayed a lineated crystal from caused by shear.

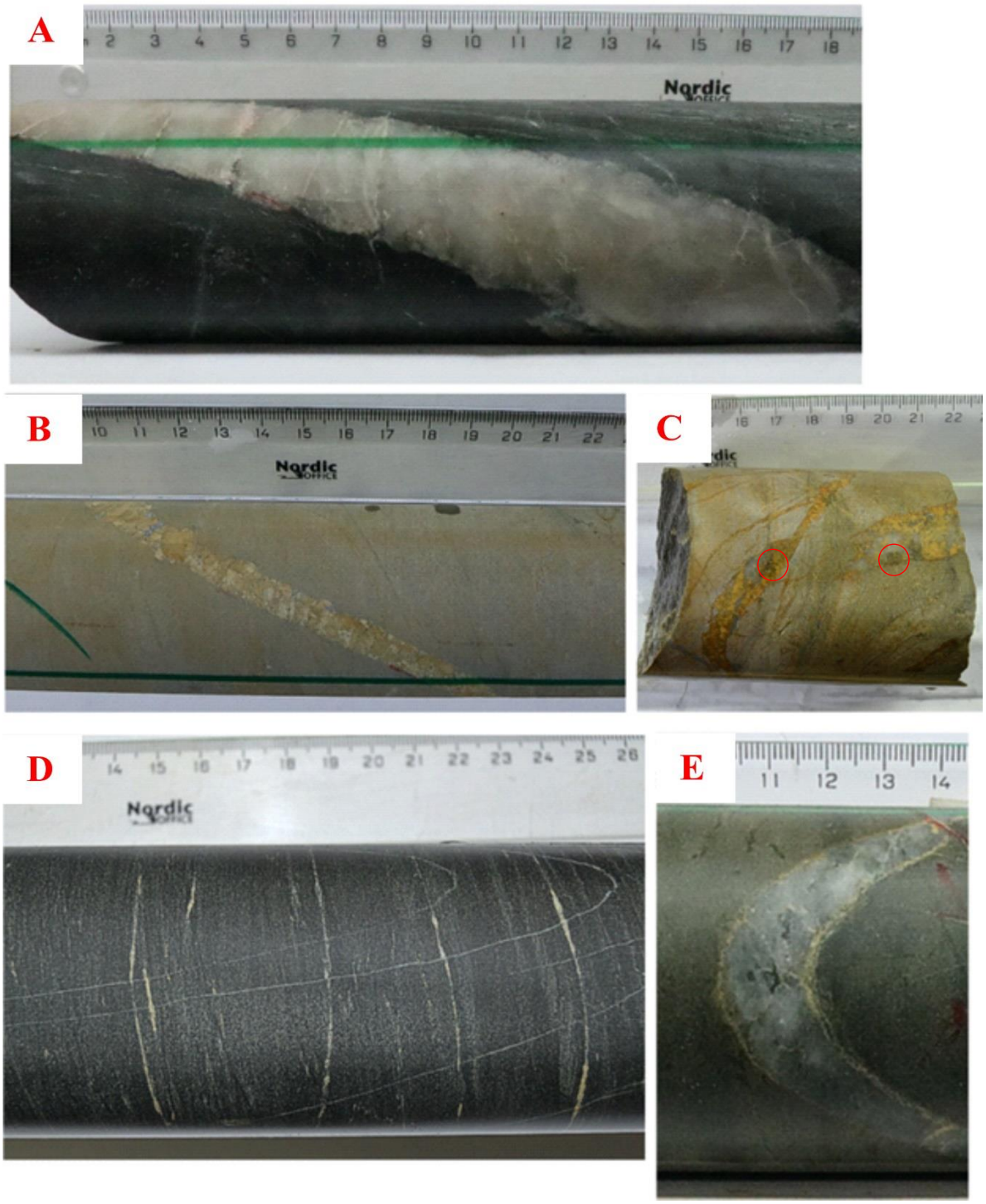

Figure 21. Figures of different vein types from varying drill cores and depths. A. Type 1 quartz vein. B. Type 2 Fe-carbonate + quartz vein. C. Type 3 Fe-carbonate + quartz + sulphide vein. Red circles point out parts with grain clustered fine grained pyrrhotite. D. Type 4 calcite vein, both cross-cutting and parallel to foliation. E. Type 5 quartz + calcite vein.

Type 1 and 5 veins have similar mineral composition, and type 1 veins may have contained calcite as fracture filling and/or contacts between the host-rock (Figure 22A, E). As the drill core is only ~5 cm wide, the lack of calcite in pure quartz vein cannot be ruled out from the whole length of the type 1

vein. Additionally, type 1 and 5 veins have mainly similar orientations. Both vein types have same three main vein orientations: 1) 360/sub-vertical, 2) 040/40, and 3) 215/25 (Figure 22, A, E). Vein orientations #2 and #3 are linked to ductile deformation features e.g., foliation and foliation parallel shear bands and zones.

Vein type 2 is the most abundantly observed with a total of 254 drill core measurements. Vein type 2 occurs in both Kati and Retu areas, but the majority of measurements, (244) were from the Kati target. Figure 22B displays moderately scattered poles to veins, but two main vein orientation sets are distinguished: 1) 360/sub-vertical, 2) and sub-vertical veins with NNW trends. Additionally, four minor vein orientation sets occur: 1) 040/30, 2) 115/75, 3) 235/45, and 4) 315/60 (Figure 22, B).

Vein type 3 is the foremost gold bearing vein type of the five. It was observed 145 times, from which 137 measurements were from Kati target. Observations from vein type 3 display two sub-vertical main orientations, dip azimuths 340 and 085 (Figure 22, C). Furthermore, a third orientation set is observed with a dip azimuth of NE and dip angle at an average of 30 degrees. Third vein orientation is moderately scattered by dip azimuth, which varies from ENE to NNE.

Type 4 vein observed 196 times, and it was detected in both Kati (145) and Retu (54) areas. Type 4 veins have three steep-angle dipping vein orientation sets: 1) 010/80, 2) 075/80, and 3) 170/70 (Figure 22, D). Veining has focused on areas of high magnitude ductile straining, which leads to steepness of the dipping angles of vein sets, but still mainly obtaining ductile deformation-parallel status of the host-rock. During the drill core investigation type 4 veins were observed abundantly as foliation parallel, but they were not measured lack of oriented drill core. These veins are most common in mafic volcanic rocks, which have not been subjected to hydrothermal alteration, other than moderate chlorite alteration. Type 4 veins are better preserved as the other vein types, which is likely due to formation in more ductile deformation phase. These veins are the thinnest (Figure 21, D) and the most abundant and they make-up the majority within the vein-density measurements per metre (appendix figures). Even though gold is precipitated in veins throughout the study area, vein type 4 does not contain gold.

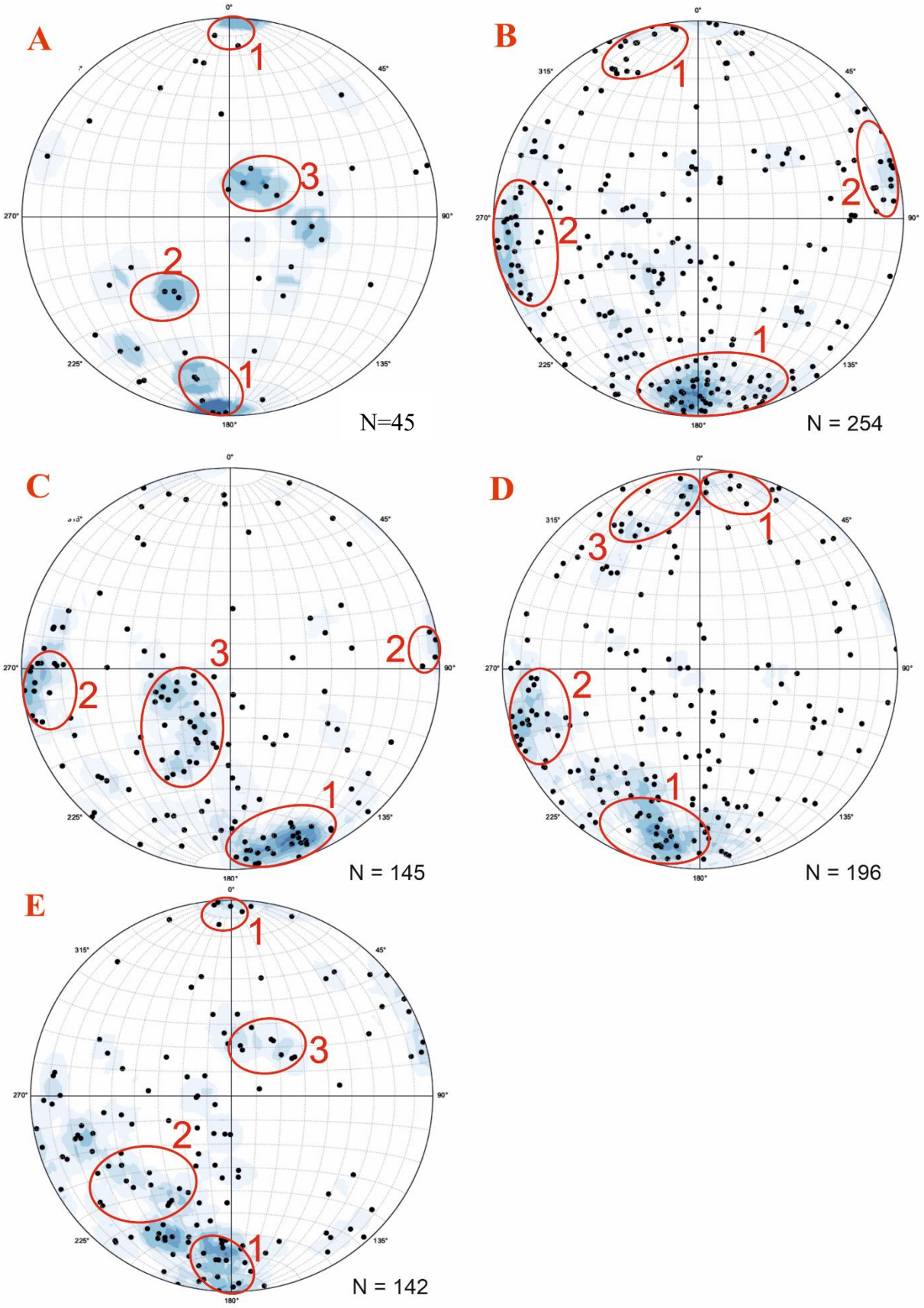

Figure 22. Stereoplots of vein types measured through the study area. A= type 1 quartz veins, B= Type 2 quartz + Fe-carbonate, C= Type 3 quartz + Fe-carbonate + sulphide, D= Type 4 calcite, E= type 5 quartz + calcite. Numbered circles display orientation sets discussed in the text.

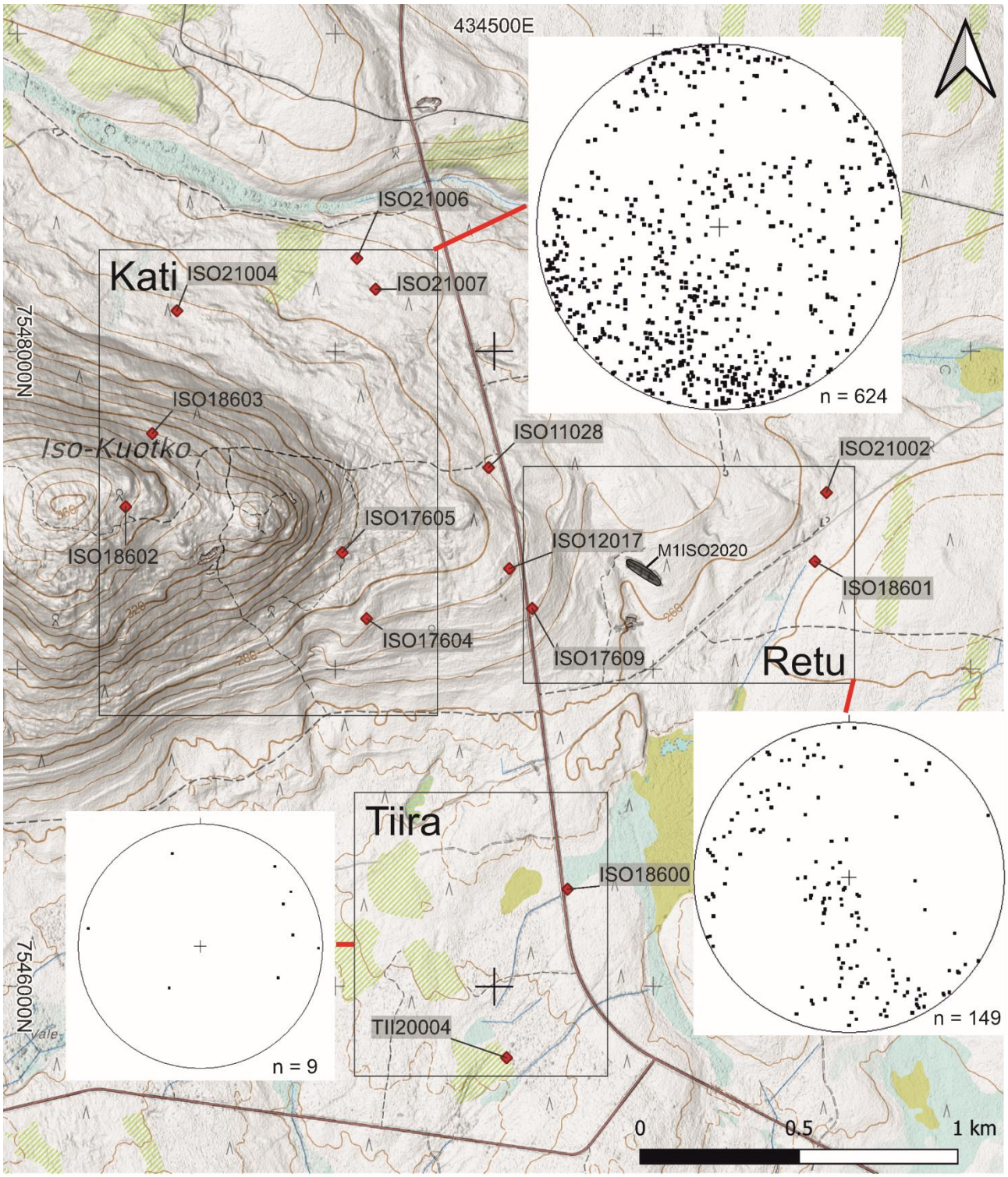

Figure 23. The study area divided into Kati, Retu and Tiira targets. Map displays exploration trench M1ISO2020 in Retu area and observed drill core and bore holes. Lower hemisphere projections display drill core vein measurements from each target.

6.4.2 Occurrences of veins in the Kati area drill holes

Drill core ISO17604, located in the central parts of the Kati area, (Figure 24) has four distinguishable vein orientations: 1) 341/85, 2) 052/85, 3) 094/25 and 4) 313/60. Gold related sulphide bearing veins occur mostly at intervals #1 and #3 at measured depth (MD) -values 112-115 m and 201-204m (Figure

24). These veins are mainly subvertical in dip and with dip azimuth towards 340 and 020. Vein interval #4 at MD236-239 m contains only non-gold bearing veins (Figure 24).

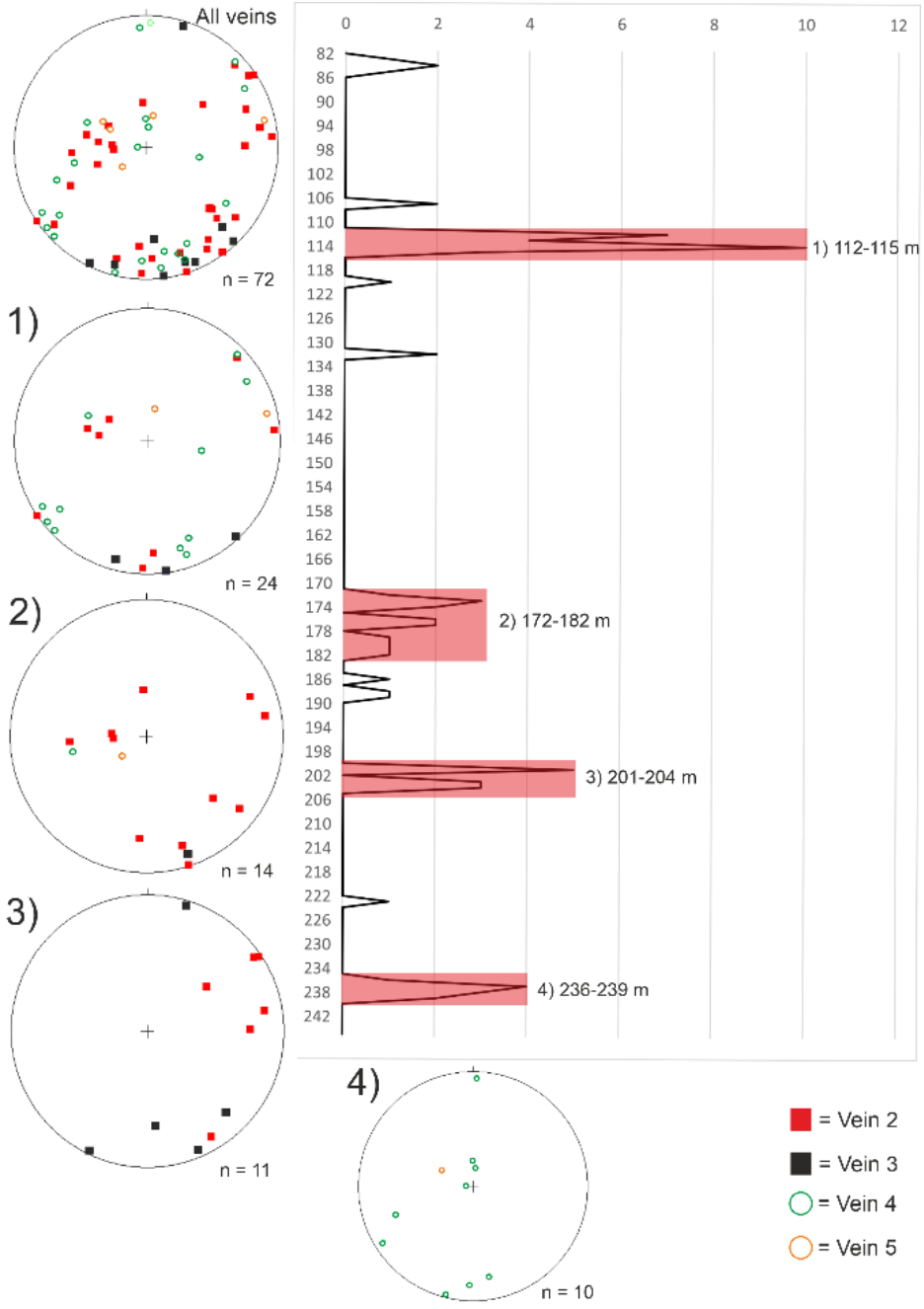

Figure 24. ISO17604 drill core vein densities and stereoplots. Horizontal axis shows the number of veins per metre along the drill hole. Measured veins are densest between 114-115 m, 172-182m, 201-204 m, and 236-239 m depths. Gold critical veins plotted as red and black squares.

Drill core ISO21004, located in northern parts of the Kati area, features four clear vein orientation sets: 1) 150/75, 2) 260/60, 3) 015/90 and 4) 345/30 (Figure 25). Sub-vertical veins occur mainly at depths below 95 meters. The more gently-dipping vein orientation set 1) observed mainly at shallower depths < 95 metres. Out of 59 vein measurements 47 are related to gold bearing types of veins. The

majority of shear bands measurements are dip towards NW, N and NE. At around 145 m depth occurs three sub-vertical E-W trending shear bands.

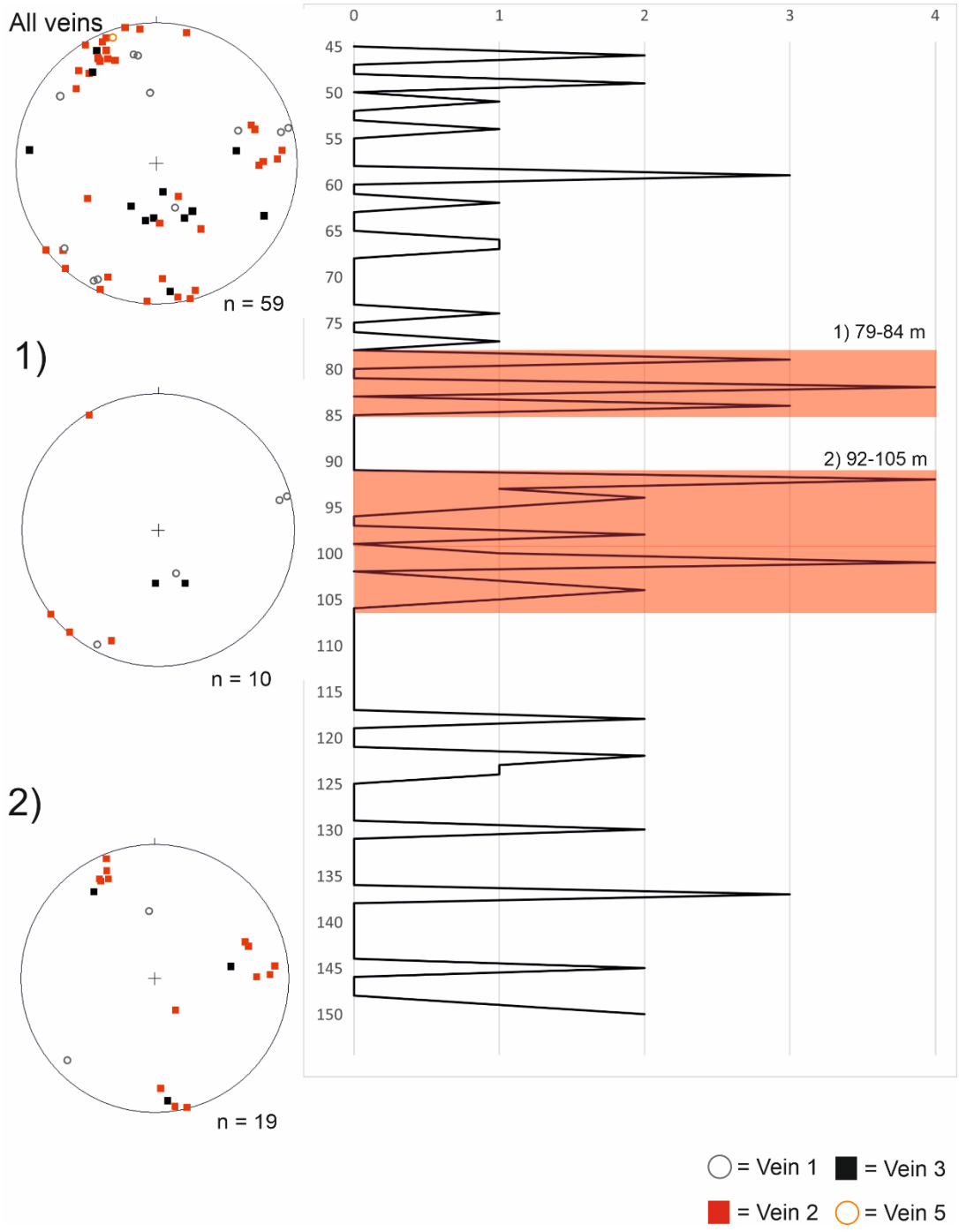

Figure 25. ISO21004 drill core vein densities and stereoplots. Horizontal axis shows the number of veins per metre along the drill hole. Measured veins are densest between, 79-84 m and 92-105 m depths. Gold critical veins plotted as red and black squares.

Drill core ISO17605 has 37 vein measurements from drill core and 274 vein measurements measured from video of the borehole (Figure 26, Figure 27). Drill core measurements indicate three vein

orientations: 1) 040/65, 2) 035/35 and 3) sub-vertical with E-W trend. No clear vein intervals could be determined from vein densities at depth (Figure 26). Vein orientations do not have a depth control.

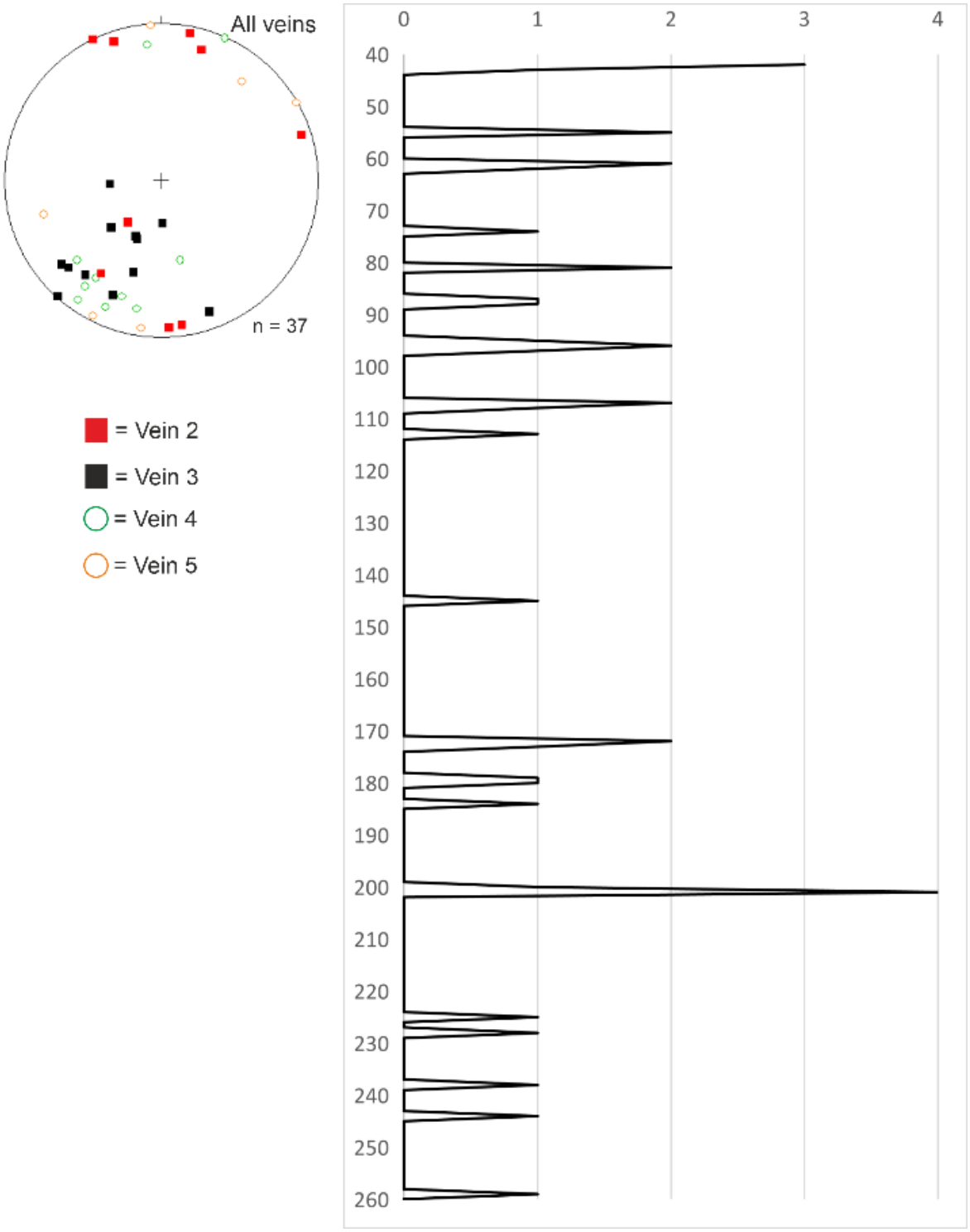

Figure 26. ISO17605 drill core vein densities and stereoplots. Horizontal axis shows the number of veins per metre along the drill hole. Gold critical veins plotted as red and black squares.

Measurements taken from bore hole video have more variable vein orientations from those measured from the drill core. Video measurements have three vein orientations: Two subvertical/vertical vein

orientations striking towards 306 and 248 and one gently-dipping vein orientation 075/25. Gold related veins appear in both subvertical and gently-dipping vein orientations (Figure 27). The vein measurements from the video have similar dip and dip direction with the drill core measurements.

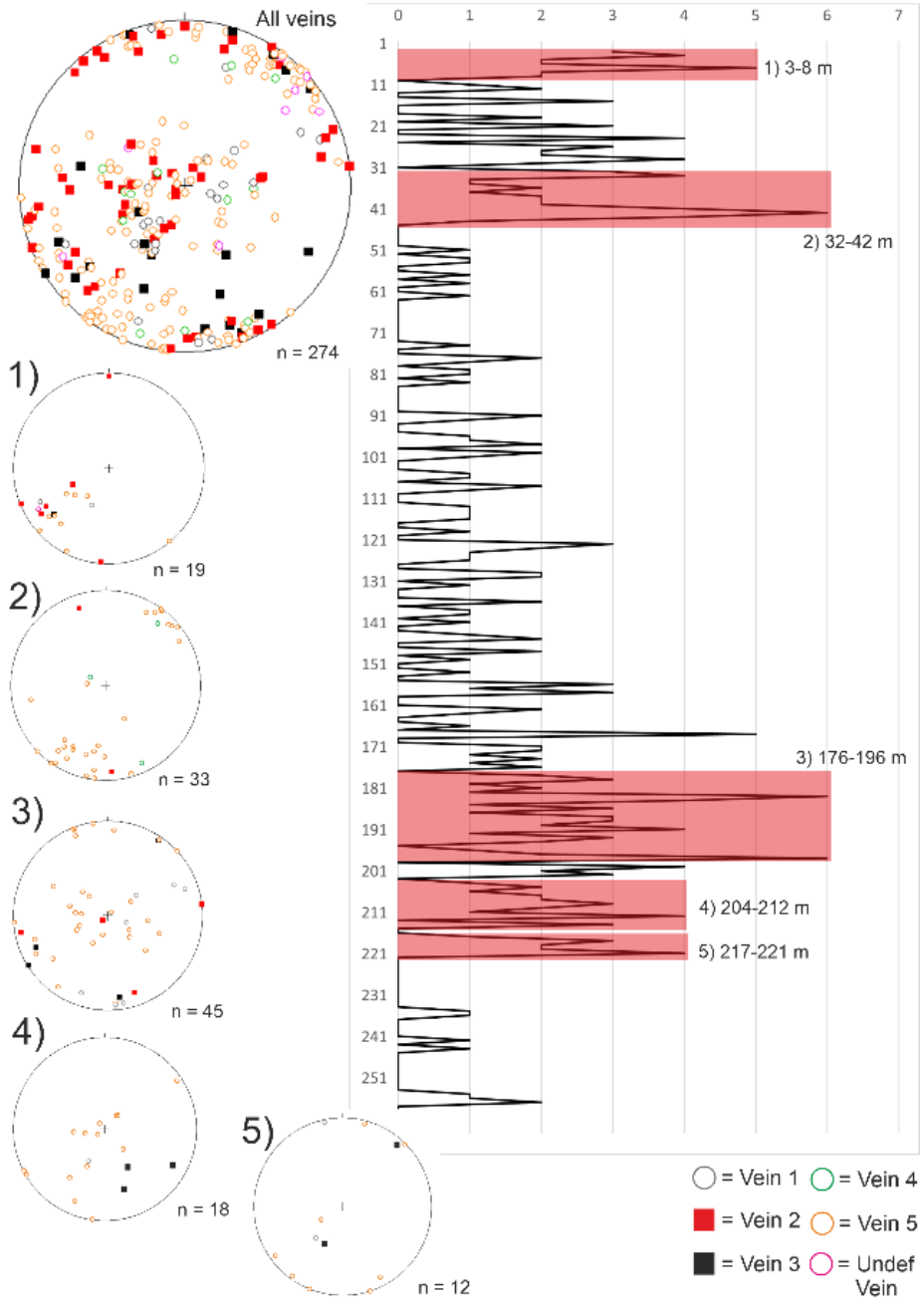

Figure 27. ISO17605 drill hole video interpretation vein densities and stereoplots. Horizontal axis shows the number of veins per metre along the drill hole. Measured veins are densest between 3-8 m, 32-42 m, 176-196 m, 204-212 m, and 217-221 m depths. Gold critical veins plotted as red and black squares.

In drill core ISO18602 (Figure 28) there are three distinguishable vein populations: 1) 074/87, 2) 002/75 and 3) 035/52. Third vein population has some deviation in dip angle between 52-40°. A lesser vein orientation set is evident dipping at an angle of 35 towards SW. It also has a perpendicular vein orientation set with dip azimuth to NE. E/W trending vein population is most apparent at vein

intervals #3, #4, #5 and #6 (Figure 28). Gold related veins are mainly featured in vein intervals #2, #3, #4 and #5. At vein interval #2, gold related vein population is at gently-dipping angle (30°), dipping towards 066. This indicates relation to foliation caused by thrusting event.

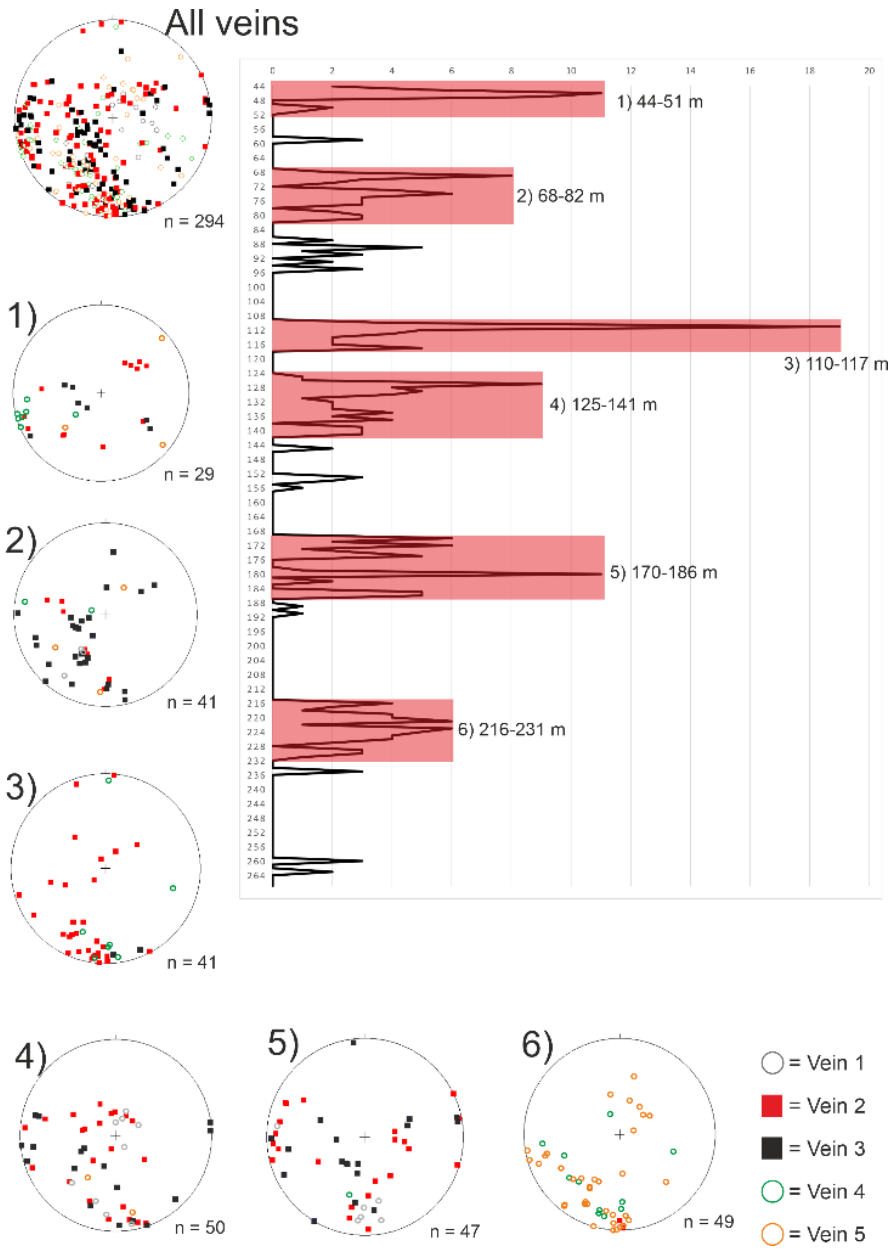

Figure 28. ISO18602 drill core vein densities and stereoplots. Horizontal axis shows the number of veins per metre along the drill hole. Measured veins are densest between 44-51 m, 68-82 m, 110-117 m, 125-141 m, 170-186 m, and 216-231 m depths. Gold critical veins plotted as red and black squares.

Drill core ISO18603 features three similar vein orientation sets as drill core 18602 (Figure 28, Figure 29). The most abundant orientation set is 085/80, with slight splay in dip azimuth. The other two vein orientation sets are 010/80 and 029/30. Notably, the latter set becomes more distinct at greater depths within vein intervals #5 and #6 (Figure 29).

Both drill cores ISO18602 and ISO18603 have several subvertical veins dipping towards NE, which scatter in dip direction (Figure 28, Figure 29).

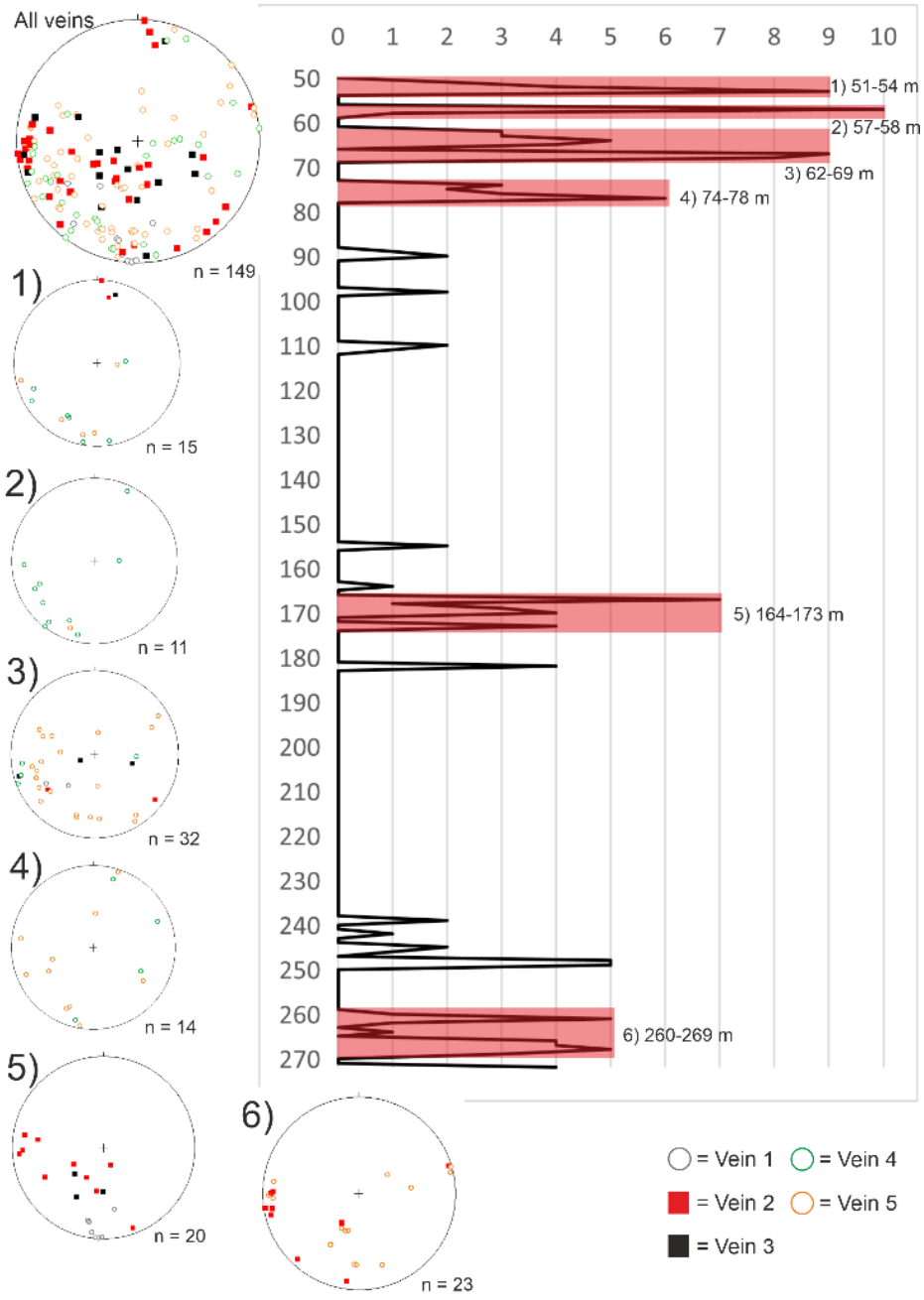

Figure 29. ISO18603 drill core vein densities and stereoplots. Horizontal axis shows the number of veins per metre along the drill hole. Measured veins are densest between 51-54 m, 54-57 m, 62-69 m, 74-78 m, 164-173 m, and 260-269 m depths. Gold critical veins plotted as red and black squares.

Drill core ISO21006 (Figure 30) has relatively limited number of vein measurements (29), but one vein orientation can still be determined; 175/80 with a ~20 degree spread towards SE in dip direction. Dip direction of dominating vein orientation is mainly perpendicular to the dominating shear band orientation. At the #1 vein interval shear band is 012/82.

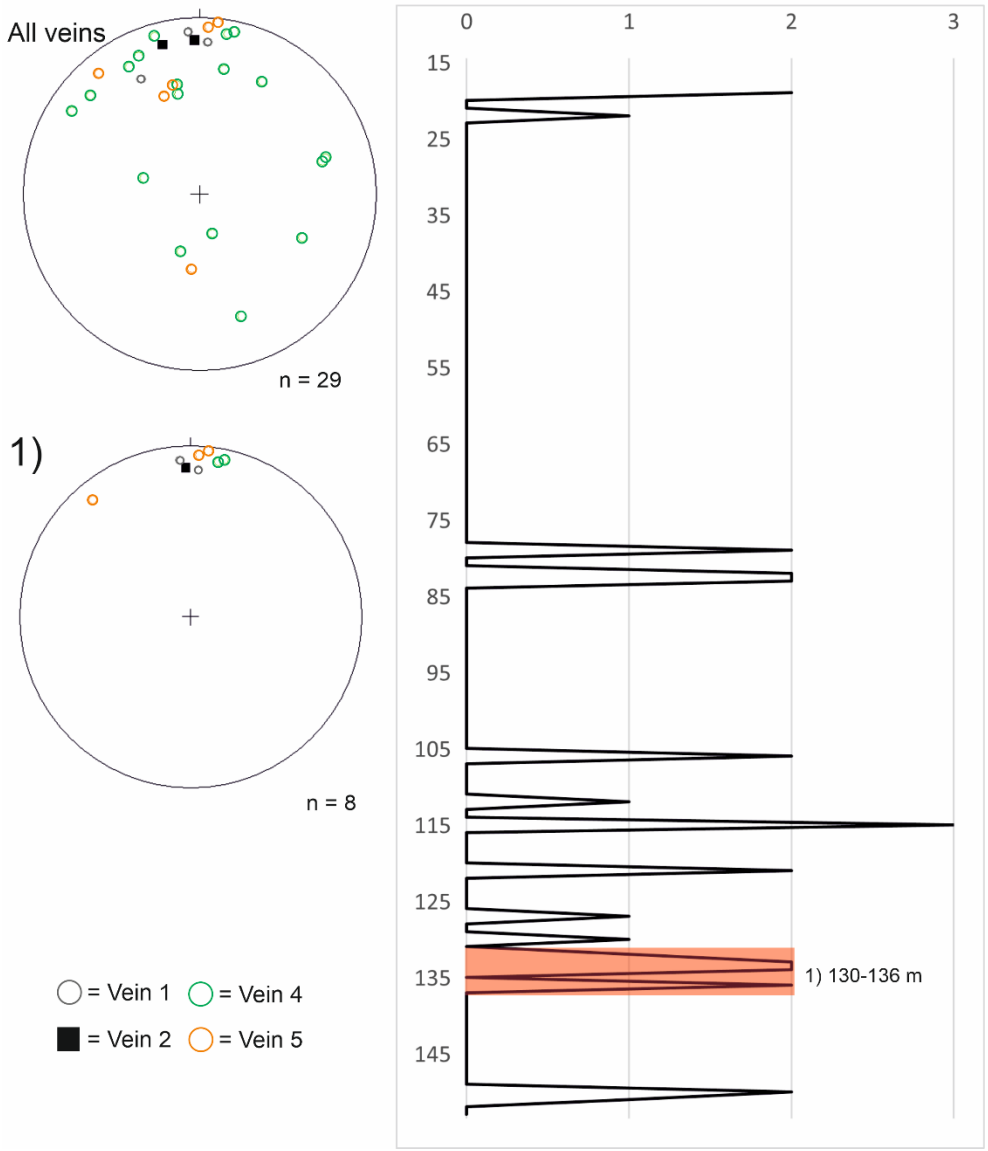

Figure 30. ISO21006 drill core vein densities and stereoplots. Horizontal axis shows the number of veins per metre along the drill hole. Measured veins are densest between 130-136 m depth. Gold critical veins plotted as black squares.

6.4.3 The dominant vein orientations in the Kati area

In conclusion, the most dominating vein orientation sets in Kati area are: 1) 075/85, 2) 005/85 and 3) 050/40 (Figure 23). Both sub-vertical vein sets have some scatter in dip direction shown by dips toward opposite directions: 1) dipping also towards 255, and 2) dipping also towards 185. The third vein set has a scatter of approximately 20 degrees in both dip direction and in dip angle. The third vein set is generally parallel to the surrounding foliation (Figure 15, blue plane), whereas the two sub-vertical vein sets have similar orientations as the Kati areas shear bands (Figure 15, red planes).

6.4.4 Occurrences of veins in the Retu area drill holes

Drill core ISO18601 has three distinguishable vein populations: 1)151/65, 2) 180/72 and 3) 013/12 (Figure 31). Vein population 1 is mostly visible at 298-300 m depth. Gold-associated veins are most prevalent within the deepest vein intervals, belonging to orientation populations 1-3.

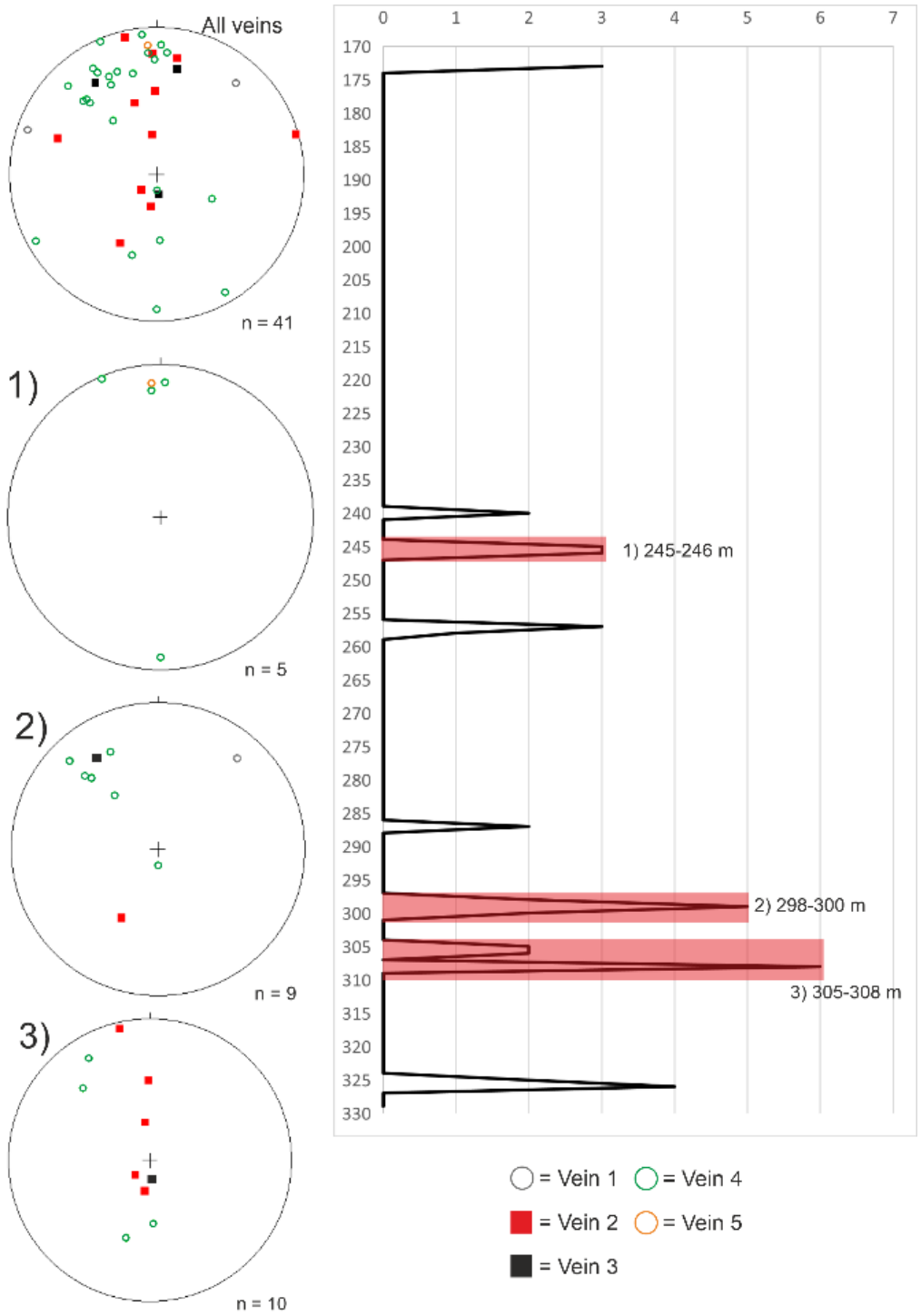

Figure 31. ISO18601 drill core vein densities and stereoplots. Horizontal axis shows the number of veins per metre along the drill hole. Measured veins are densest between 245-246 m, 298-300 m, and 305-308 m depths. Gold critical veins plotted as red and black squares.

Drill core ISO17609 reveals the presence of three dominant vein orientations, with the clearest being 337/78 (Figure 32). The dip direction of the vein orientation varies within approximately 20 degrees. The other two vein orientations are subvertical and sub horizontal, both of which dip towards the east (090). Between depths of 96-108 m, a vein concentration is observed, encompassing 31 measured veins. This interval includes the most prominent WNW-dipping vein orientation, as well as the sub-horizontal and sub-vertical vein orientations. Veins belonging to the gold-bearing types are primarily oriented in the 337/78 direction and the 120/80 direction.

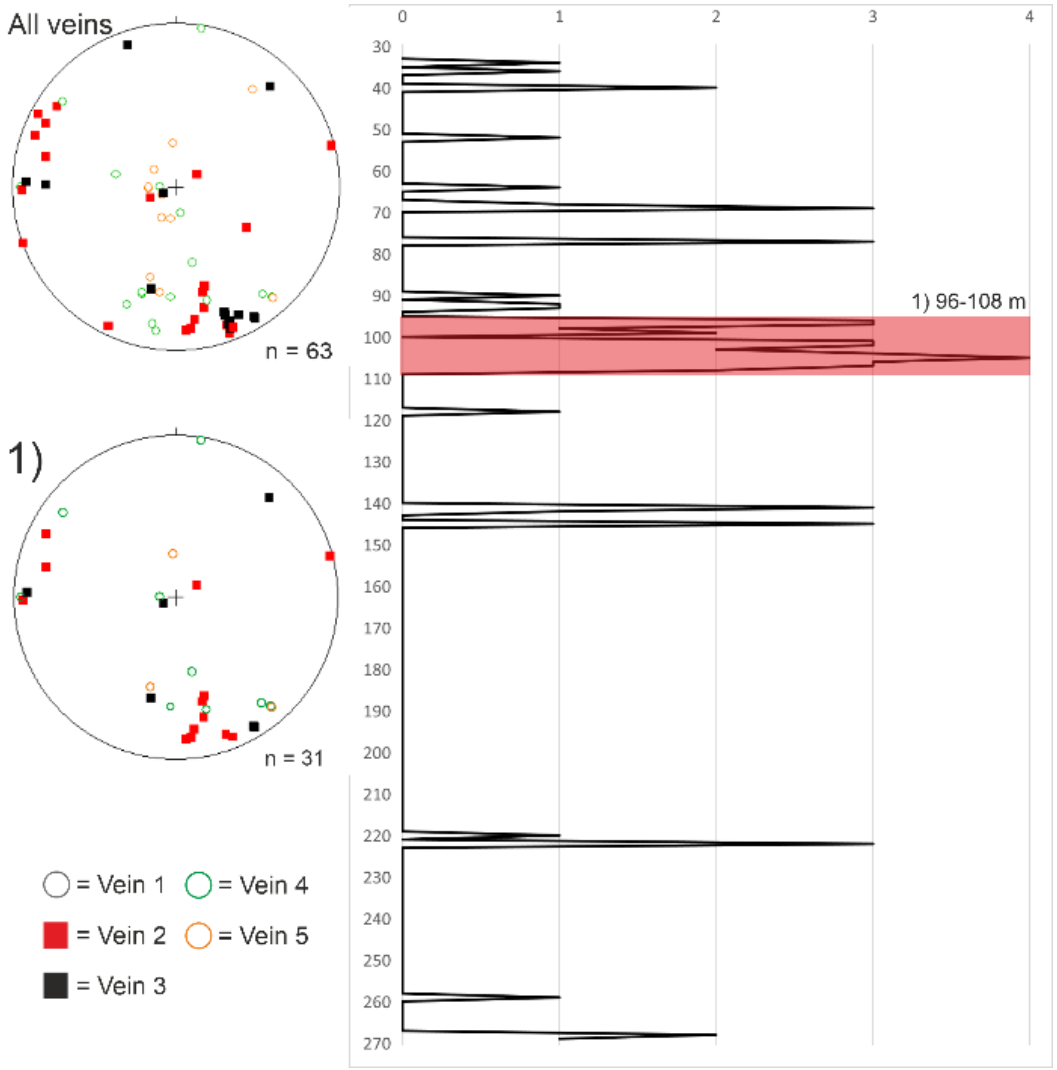

Figure 32. ISO17609 drill core vein densities and stereoplots. Horizontal axis shows the number of veins per metre along the drill hole. Measured veins are densest between 96-108 m depth. Gold critical veins plotted as red and black squares.

6.4.5 The dominant vein orientations in the Retu area

In summary, the most dominant vein orientations in Retu area are: 1) 335/80, 2) 050/08, 3) 110/80, and 4) 150/65 (Figure 23). Subhorizontal veins are likely foliation parallel, which was observed in exploration trench investigation (Figure 11, A). Two other dominant vein orientations are likely due to the local subvertical shear band (Figure 15).

6.4.6 Tiira

Tiira target is situated within the Kiistala shear zone which has been later reactivated by Suaspalo Post-glacial fault. Therefore, limited structural measurements were undertaken due to the fragmented nature of the drill core, primarily composed of rubble caused lost likely by Suaspalo Post-glacial fault. Foliation and shear features were dipping sub-vertical towards NNW. Only five measurements of vein type 4 could be taken, with an approximately 240/65 average orientation.

6.5 Comparison of structure orientations between targets

Foliation in all targets is varying from one another. Kati area's foliation is mainly dipping ~40 degrees towards E and NE, whereas Retu area is mainly subhorizontal undulating towards N and S. Foliation in Tiira area is sub-vertical due to KiSZ.

In both, Kati and Retu locations, two sub-vertical vein orientations are observed (Figure 33). However, they have different strike between the targets, in Kati trend mostly towards NW-SE and ENE-WSW, and in Retu towards NE-SW. Additionally, in both areas one vein orientation set is parallel to the prevailing foliation.

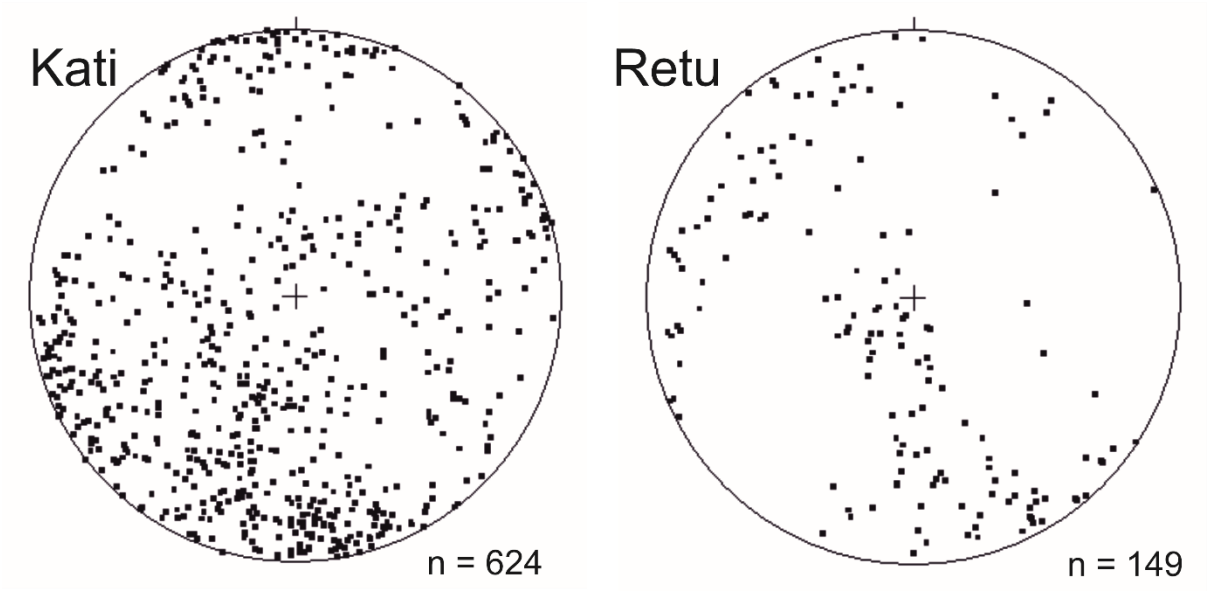

Figure 33. Rose plots of vein measurements from Kati and Retu area. Rose plots display dominant dip direction.

In drill cores: ISO17604, ISO17605, ISO17609, ISO18602, ISO18603 and ISO21004 (Kati target) where shear bands are gentle in dip, the close by gold critical veins are dominantly sub-vertical. The drill cores ISO18603 and ISO21004 have both sub-vertical and shear parallel vein orientations. In drill core ISO18601 from Retu target at 308 measured depth the gently-dipping gold bearing veins are dominantly parallel or sub-parallel to the surrounding shear bands.

6.6 Optical imaging

Using the optical drill holes imaging method, a total of three boreholes were investigated, namely: ISO11028, ISO12017, and ISO17605. The videos yielded measurements predominantly of foliation, fractures, and veins, though identifying the veins posed a challenge. The challenge in identifying the veins was caused from the sediment deposition within the boreholes. Measurement results were obtained throughout the entire length of the borehole. Drill hole ISO17605 results are displayed above (Figure 27), since it was compared with the drill core measurements observed from the same hole.

Drill core ISO12017 and ISO1128 are located in between Kati and Retu areas. In reference to the finding presented in Figure 34, a total of 518 structural measurements have been acquired from borehole ISO11028. Measurements focus primarily on veins composed of quartz and quartz + calcite. Despite the measurements exhibiting scatter, three distinct vein populations are identified: 1) sub-vertical veins with dip directions varying between 070 and 250, 2) 055/40, and 3) 130/75.

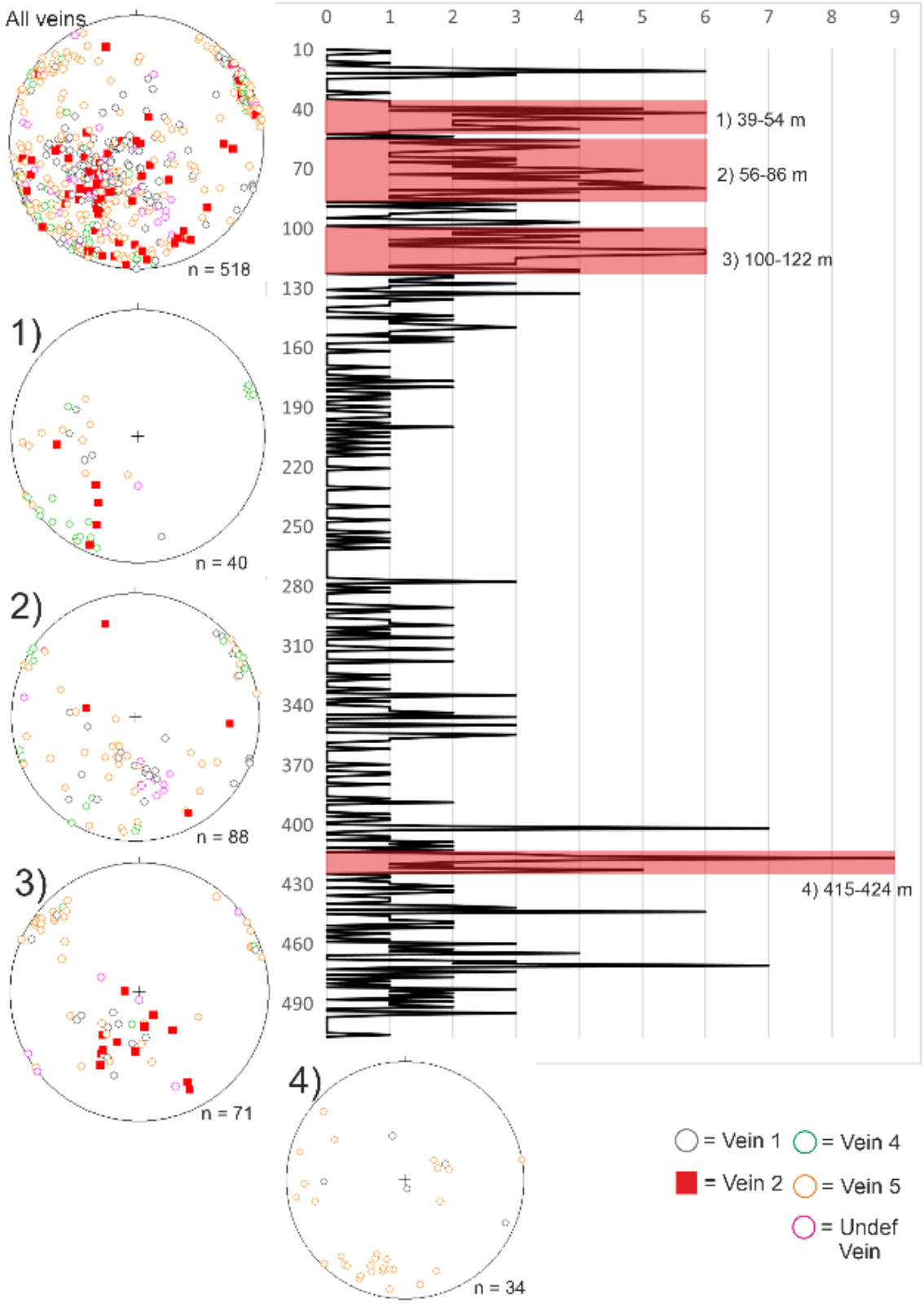

Figure 34. ISO11028 borehole imaging measurements. Horizontal axis shows the number of veins per metre along the drill hole. Measured veins are densest between 39-54 m, 56-86 m, 100-122 m, and 415-424 m depths. Gold critical veins plotted as red squares.

Drill core ISO12017 contains three main vein orientations (Figure 35): 1) dip azimuth undulating sub-horizontal, 2) sub-vertical NE dipping and 3) sub-vertical NW dipping vein set. Additionally, two minor 50-degree dipping vein set are distinguished, one dipping towards SE and the other NNW.

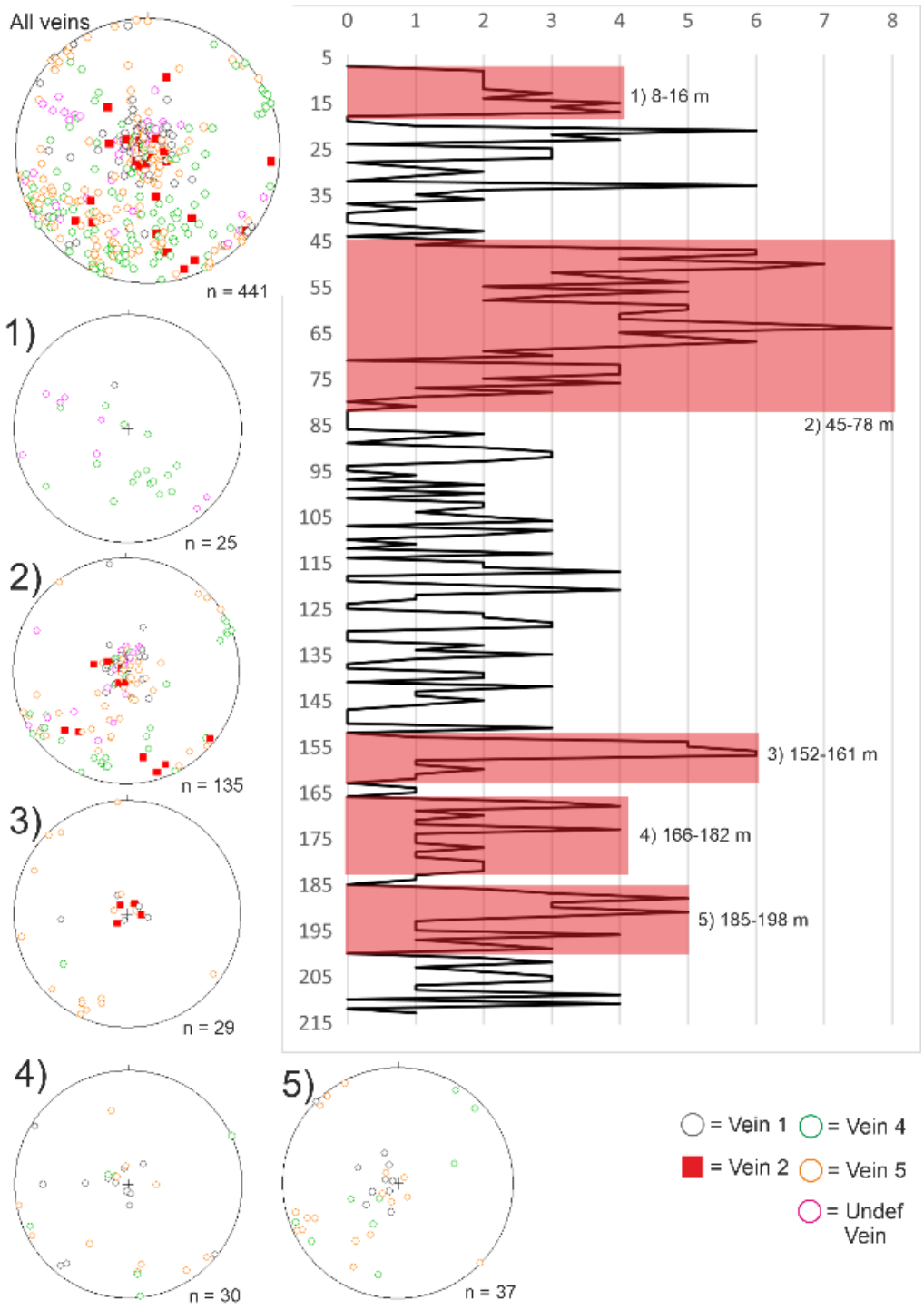

Figure 35. ISO12017 borehole imaging measurements. Horizontal axis shows the number of veins per metre along the drill hole. Measured veins are densest between 8-16 m, 45-78 m, 152-161 m, 166-182 m, and 185-198 m depths. Gold critical veins plotted as red squares.

7. Discussion

7.1 Regional scale ductile deformation features

Interpreting the results, the KiSZ (Figure 36) aligns with Niiranen (2015) description of a thrust zone that has later activated as the KiSZ/RuSZ. In specific, the predominantly gently NE-dipping foliation reflects the thrust zone resulting from the collision of the Lapland Granulite Belt with CLB from the NE (Figure 5, C). Patison (2007) and Sayab et al. (2019) studies support this interpretation. Drill core measurements confirm that KiSZ is a sub-vertical structure. This interpretation is supported by Sayab et al. (2019) analysis of CLB's development. The NNW-trending structural line on the western side of the Kati area (Figure 10) possibly represents demagnetized thrust faults or a cluster of right-handed conjugate faults associated with the left-handed KiSZ.

In the northern part of the Kati area, the E-W trending trend line correlates with the N and NE dipping foliations observed in drill core measurements, compatible with the northern limb of a NE-plunging fold. KiSZ could constrain the southern limb of the fold. Alternatively, the fold axis may plunge towards NNW, with the Kapsajoki Dz (Figure 10) causing deformation on the western limb of the fold extending further west from the Kati-Retu areas.

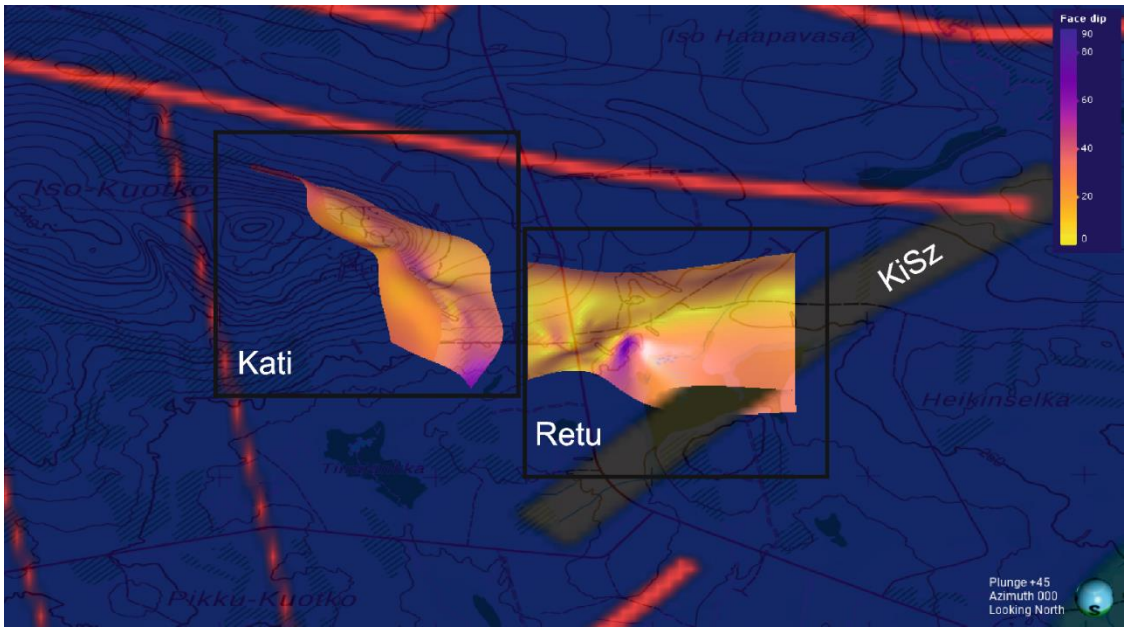

Figure 36. Ductile geometries (orange to purple colour) of Kati (left) and Retu (right) and structural trend lines (red lines) interpreted from magnetic geophysical image. Kapsajoki Dz trends NNW in the west outside of this map.

In the Retu area, the dominating sub-horizontal foliation likely reflects the layering of volcanic rocks (S0). There is a challenge in placing this sub-horizontal foliation in the complex deformation of the CLB. The correlation between sub-vertical left-handed shear structure and the interpreted KiSZ trend line indicates a connection between the two (Figure 11, A, C, Figure 14), suggesting a parallel

relationship between the “synthetic” R shear fractures or shear bands and the shear zone measured from the trench and (Figure 11) KiSZ.

7.2 Shear features

In both areas, shear structures are in parts aligned with the main foliation and are spatially associated with gold-bearing quartz-carbonate-sulfide veins. The veins occur preferentially within shear zones as the shearing was associated with formation of fractures creating pathways for gold enrichment. The relationship between gently-dipping and sub-vertical shear structures remains unknown.

The gently-dipping shear structures in the Kati area align with previously suggested NW-trending shear bands (Patison, 2001; 2007), possibly indicating initially gentle thrust faults that later tilted sub-vertically. The NE and ENE trending shear bands in the Kati area (Figure 15, Kati, red planes) might be left-handed conjugate shears (Figure 17) associated with right-handed NW shear features.

There are more sub-vertical shear bands in the Kati area compared to the Retu area. Härkönen et al., (2000) suggests that veining in Kati forms horse-tail type quartz + carbonate bearing vein swarm. Based on this, the Kati area vein swarms have formed within shear bands. Also, Molnár et al., (2018) study reveals that there are more local shear bands in Kati compared to Retu. The few NE trending shear features measured from Tiira target correlate with the trend of KiSZ.

7.3 Veins

7.3.1 Appearance

The veins across all types display undulating and/or sheared features, suggesting formation during or before the latest deformation phase. Type 4 veins have the most sheared veins; therefore, it represents the earliest vein type. Additionally, they are not gold bearing and are in many cases cross-cut by other vein types.

Vein types 1 and 5 are relatively similar with respect to their mineral composition, and orientations (Figure 22, A, E). These veins are on average the widest of the vein types, which suggests that they have formed in the widest of fractures caused by shear zones/bands, most likely within shear zones.

Vein types 2 and 3 have similar mineral composition and orientations, likely indicating synchronous formation. These veins are typically found in albitized and/or sericitized mafic volcanic rocks and felsic dikes. Mafic volcanic rocks may have undergone albite and sericite alteration in earlier deformation phase compared to gold-enriching deformation phase. According to Sayab et al. (2019), the area has experienced four distinct deformation phases before the final, fifth deformation phase,

believed to be the gold enrichment phase in Iso-Kuotko (Molnár et al., 2018). Brittle deformation structures serve as effective pathways for fluid migration as well as barriers for fluid enrichment.

7.3.2 Orientations

Veins can be broadly categorized into sub-vertical E-W trending, sub-vertical NW-SE trending, and moderately NE-dipping sets. These orientations align well with the sub-vertical shear bands and the gently N to E dipping foliation in the Kati area. While there are fewer measurements for sub-vertical shear bands in the Retu area, vein of types 2, 3, 4, and 5 show orientations correlating with the sub-horizontal cleavage in the area. Type 2 and 3 veins with two sub-vertical vein orientations can be linked to steeply-dipping strike-slip shear. Differences in dip azimuth between the targets are likely due to variation in shear band orientation.

The vein orientations observed in drill core ISO17604 provide a clear representation of typical orientations within the Kati target, as they are relatively aligned with the area's shear elements. Most gold-critical veins are located at depths below 230 meters, but some sub-vertical gold-critical veins additionally occur within the middle depths of the drill core, ranging from 172 to 204 meters.

Drill core ISO21004 from north of Kati area exhibits largely similar features regarding gold-critical veins as other drill holes in the Kati area, with veins ranging from sub-vertical to gently-dipping in the direction of the foliation (Figure 25). In contrast to the more southern Kati drill cores, the gently-dipping veins dip towards the north instead of the typical northeastern dip. The northerly dip correlates with the modelled foliation surface, which turns from the northeast to north in the northern part of the Kati area. An exception is the population of the sub-vertical veins, which dip to the southeast. As these are not parallel to local shear elements, they likely represent conjugate fractures associated with a gently north-dipping foliation. These measurements are supported by drill core ISO21006, also located in the northern part of the Kati area. In both drill holes, sub-vertical veins are predominantly found at depths below 90 meters.

In drill core ISO17605 in the middle of the Kati area (Figure 26), gold crucial veins are sub-vertical and oriented either E-W or gently-dipping along the prevailing cleavage. The sub-vertical veins correlate with shear elements measured from the drill core. This suggests that the veining in the area is controlled by the the network of localized high-strain deformation structures. The orientations of the other vein types are similar with those of the gold-critical ones. Video imaging of the bore hole proved to be a valid method for measuring structures and veins, as it correlates quite well with the directions measured from the drill core (Figure 26, Figure 27). Video imaging allows for a much more comprehensive measurement of structures compared to the drill core.

Drill cores ISO18602 and ISO18603 from western side on the Kati area are approximately 200 meters apart, with the latter being to the north, and the measured veins in both drill cores are mostly oriented in the same direction. In drill core ISO18602, gold-critical veins are located at depths below 216 meters, while in drill core ISO18603, they are predominantly at depths deeper than 175 meters. This confirms that veins essential for gold occur, at least locally, along specific horizons which continuation is controlled by the gently-dipping (045/30) foliation, as the northern gold-critical veins are deeper than those in the southern part. In both drill cores, non-gold-critical veins are generally oriented similarly to the gold-critical veins, but they are at different depths from each other. The depth variation within vein types may result from differences in lithology or variations in the intensity of the host rock alteration.

The veins in two drill holes studied in the Retu area are mainly oriented in the direction of the dominating sub-horizontal foliation, as well as two sub-vertical vein orientations trending in the NE-SW and N-S. The veins in drill core ISO18601 trend E-W, but their dip varies from sub-horizontal to sub-vertical. Gold-critical veins, according to the results, are mainly present from a depth of 298 meters downward. Drill core ISO17609 is located at the western edge of the Retu area near the Kati area, and it displays a sub-vertical NE trending population of gold-critical veins with similar features to the gold-critical vein population in the Kati area.

In both Kati and Retu areas, the primary vein orientations are sub-vertical, but dip directions differ relative to each other. The sub-vertical veins in the Kati area trend NW-SE and ENE-WSW, whereas those in the Retu area trend NE-SW (Figure 33). The orientation of sub-vertical veins in the Retu area is influenced by KiSZ and possible deviating conjugate fractures from KiSZ. In contrast, the orientation of sub-vertical veins in the Kati area is controlled by NW-trending shear structures originating from KiSZ and the local reactivation of NE-dipping thrust faults into sub-vertical thrusts. Both areas also display vein orientations parallel to the prevailing foliation, with mean orientations of 050/40 within the Kati and 050/08 within the Retu.

Optical imaging of the studied boreholes provides comprehensive results, especially for boreholes ISO12017 and ISO11028. These boreholes are located between the Kati and Retu areas, and there is no other measurement data available for this study from this area. The main orientation trends of vein measurements in borehole ISO12017 align with those in the Retu area, particularly in terms of sub-horizontal and sub-vertical vein orientations. On the other hand, the vein measurement results in borehole ISO11028 correlate with the main vein orientations in the Kati area, including a foliation oriented gently-dipping NE trend and three distinct sub-vertical vein orientations with strikes of N,

NE, and E. Consequently, the differences in vein orientations between the Kati and Retu areas are variable, and no clear boundary was identified.

8. Conclusions

Generally, the ductile deformation structures e.g., foliation and folding interpreted in this study correlate with previous studies in the region (Patison, 2000, 2001; Niiranen, 2015). The structural character of the area is dominated by KiSZ, which according to earlier structural interpretations (Niiranen, 2015; Sayab et al., 2019), was initiated as a thrust zone that re-activated as a left-handed sub-vertical strike-slip shear zone. The rocks in the Kati area are foliated, gently-dipping mainly towards NE. According to this study, the Kati area is folded, with the fold axis plunging sub-horizontally either towards NNW or NE. The most dominant shear zone in the Kati area trends parallel to the foliation (045/30). Additionally, there are local sub-vertical shear zones and bands in the area. According to Patison (2001), the NW-trending shear bands in the Kati area are right-handed. Therefore, it can be suggested that the NW-trending shear bands of this study represent right-handed conjugate shear bands to the left-handed KiSZ. Sub-horizontal foliation in the Retu area is cross-cut by the NE-trending sub-vertical KiSZ and shear bands that are parallel to the main KiSZ. There is no clear structural boundary between the Kati and Retu areas.

Drill cores in Tiira area consists mainly of mafic volcanic rock rubble, making it challenging to obtain measurements from drill cores extensively enough to interpret the geometry of the structures. The brittle nature of the drill cores in the area is caused by KiSZ, which has been later activated by NE trending Suaspalo post-glacial fault. In this study, it was not possible to gather data systematically from kinematic markers of either ductile or brittle shear features. This prevented interpretation of the movement senses of deformation structures. For later studies, more thorough measurements from drill core data considering lineations and kinematic indicators as well as structural interpretation of kinematic indicators from thin sections are suggested.

Mineralogically five different vein types were observed and interpreted in the study area: 1) quartz, 2) quartz + Fe-carbonate, 3) quartz + Fe-carbonate + sulphide, 4) calcite, and 5) quartz + calcite. Vein type #4 has formed first, as it does not carry gold and is generally cross-cut by other vein types. The veins in both areas, Kati and Retu, are controlled by foliation parallel shearing. In Kati with an average orientation of 045/40 and in Retu with sub-horizontal with undulating dip direction mainly towards N and NE. Both areas also contain sub-vertical veins controlled by strike-slip shear bands and zones.

The results of optical video interpretation of drill cores are significantly more comprehensive than those obtained from drill core measurements. The measurements from drill core and optical video measurements correlate with each other. The difficulty with borehole video interpretation is that vein types are hard to identify, and the dirt in the water of the drill cores may blur the image, making it difficult to measure structures. In further studies, borehole imaging of several adjoining drill holes for precise and comprehensive deformation structure and vein data would help interpret vein and deformation continuities from drill core to drill core.

Broad scale interpretations of deformation structures and trend lines conducted from aeromagnetic survey data could be continued in further studies by interpretations made from more regional scale low-altitude or ground magnetic survey data.

9. Acknowledgements

I would like to thank professor Pietari Skyttä, PhD, for supervision, endless support, advice and reviewing through this project. I am grateful to have had such a great professor in structural geology.

Also, I would like to thank Project Manager Jari Ylinen for the opportunity to conduct research on the Iso-Kuotko area as well as for support and guidance. I am especially grateful for Senior Exploration Geologist Pekka Kämäräinen for teaching me a whole lot about mineral exploration and for supervising this project. For funding and working environment I'm thankful for Agnico Eagle Finland Oy.

I have had the privilege to meet many driven co-workers, who have taught me a great deal of geology and working as a team. I am grateful for each of the encounters and friendships.

Lastly, I'm grateful for my fiancé Ida for pushing me to finish this project, believing in me and for infinite support.

10. References

Bons, P.D., Elburg, M.A., Gomez-Rivas, E., 2012. A review of the formation of tectonic veins and their microstructures. Journal of Structural Geology 43, 33–62.

Eilu, P. (ed.)), 2012. Mineral deposits and metallogeny of Fennoscandia, Geological Survey of Finland Special Paper 53.

Eilu, Pasi., 2015. Overview on Gold Deposits in Finland. In: Maier, W.D., Lahtinen, R., O'Brien, H. (Eds.), Mineral Deposits of Finland. Elsevier, 377–410.

Fossen, H., 2010. Structural Geology, 1st ed. Cambridge University Press.

Goldfarb, R.J., Groves, D.I., 2015. Orogenic gold: Common or evolving fluid and metal sources through time., Lithos.

Goldfarb, R.J., Groves, D.I., Gardoll, S., 2001. Orogenic gold and geologic time: a global synthesis, Ore Geology Reviews.

Groves, David I, Goldfarb, R.J., Knox-Robinson, C.M., Ojala, J., Gardoll, S., Yun, G.Y., Holyland, P., 2000. Late-kinematic timing of orogenic gold deposits and significance for computer-based exploration techniques with emphasis on the Yilgarn Block, Western Australia, Ore Geology Reviews.

Groves, D.I., Santosh, M., Goldfarb, R.J., Zhang, L., 2018. Structural geometry of orogenic gold deposits: Implications for exploration of world-class and giant deposits. Geoscience Frontiers 9, 1163–1177.

Hanski, E., Huhma, H., 2005. Central Lapland Greenstone Belt. In: Lehtinen, M., Nurmi, P.A., Rämö, O.T. (Eds.), Precambrian Geology of Finland – Key to Evolution of the Fennoscandian Shield. Elsevier, 139–194.

Härkönen, I., 1994. Tutkimustyöselostus Kittilän kunnassa valtausalueilla Kuotko 6 (kaiv.rek.n:o 4417/1) ja Kuotko 7 (kaiv.rek.n:o 4417/2) suoritetuista malmitutkimuksista. johdanto, gtk.

Härkönen, Ilkka., Pankka, Heikki., Rossi, Seppo., 2000. Summary report, The Iso-Kuotko gold prospects, Northern Finland.

Hölttä, P., Väisänen, M., Väänänen, J., Manninen, T., 2007. Paleoproterozoic metamorphism and deformation in Central Lapland, Finland. In: Ojala, V. (Ed.), Gold in the Central Lapland Greenstone Belt. Geological Survey of Finland, 269.

Huhma, H., Hanski, E., Kontinen, A., Vuollo, J., Mänttäri, I., Lahaye, Y., 2018. Sm–Nd and U–Pb isotope geochemistry of the Palaeoproterozoic mafic magmatism in eastern and northern Finland. Geological Survey of Finland, Geological Survey of Finland, Bulletin. Geological Survey of Finland.

Köykkä, J., Lahtinen, R., Huhma, H., 2019. Provenance evolution of the Paleoproterozoic metasedimentary cover sequences in northern Fennoscandia: Age distribution, geochemistry, and zircon morphology. Precambrian Research 331.

Kramer Bernhard, J., Barnett, W., Uken, R., Myers, R., 2020. Chapter 7: Structural Analysis of Drill Core for Mineral Exploration and Mining: Review and Workflow Toward Domain-Based 3-D Interpretation. Applied Structural Geology of Ore-Forming Hydrothermal Systems 215–245.

Lahtinen, R., Huhma, H., Sayab, M., Lauri, L.S., Hölttä, P., 2018. Age and structural constraints on the tectonic evolution of the Paleoproterozoic Central Lapland Granitoid Complex in the Fennoscandian Shield. Tectonophysics 745, 305–325.

Lehtonen, M., Airo, M.-L., Eilu, P., Hanski, E., Kortelainen, V., Lanne, E., Manninen, T., Rastas, P., Räsänen, J., Virransalo, P., 1998. Kittilän vihreäkivialueen geologia: Lapin vulkaniittiprojektin raportti = Summary, the stratigraphy, petrology, and geochemistry of the Kittilä greenstone area, northern Finland, a report of the Lapland Volcanite Project. Geological Survey of Finland.

Molnár, F., Middleton, A., Stein, H., ÒBrien, H., Lahaye, Y., Huhma, H., Pakkanen, L., Johanson, B., 2018a. Repeated syn- and post-orogenic gold mineralization events between 1.92 and 1.76 Ga along the Kiistala Shear Zone in the Central Lapland Greenstone Belt, northern Finland. Ore Geology Reviews 101, 936–959.

Mutanen, T., Huhma, H., 2001. U-Pb geochronology of the Koitelainen, Akanvaara and Keivitsa layered intrusions and related rocks.

Niiranen, T., 2015. A 3D structural model of the central and eastern part of the Kittilä terrane.

Nironen, M., 2017. Structural interpretation of the Peräpohja and Kuusamo belts and Central Lapland, and a tectonic model for northern Finland. Geological Survey of Finland, Report of Investigation 234 1–53.

Patison, N.L., 2007. Structural controls on mineralisation in Central Lapland Greenstone Belt. In: Ojala, J. (Ed.), Gold in the Central Lapland Greenstone Belt. Special Paper 44. Geological Survey of Finland, 107–124.

Patison, N.L., 2001. Structural and fluid chemical controls on gold mineralisation in the central Lapland greenstone belt, northern Finland. report 2.

Patison, N.L., 2000. structural and fluid chemical controls on gold mineralisation in the central Lapland greenstone belt, northern Finland. 2000 field report.

Rastas, P., Huhma, H., Hanski, E., Lehtonen, M.I., Härkönen, I., Kortelainen, V., Mänttäri, I., Paakkola, J., 2001. U-Pb isotopic studies on the Kittilä greenstone area, central Lapland, Finland. In: Vaasjoki, M. (Ed.), Radiometric Age Determinations from Finnish Lapland and Their Bearing on the Timing of Precambrian Volcano-Sedimentary Sequences Edited by Matti Vaasjoki Geological Survey of Finland. Geological Survey of Finland, 279.

Sayab, M., Miettinen, A., Aerden, D., Karell, F., 2017. Orthogonal switching of AMS axes during type-2-fold interference: Insights from integrated X-ray computed tomography, AMS, and 3D petrography. Journal of Structural Geology 103, 1–16.

Sayab, M., Molnár, F., Aerden, D., Niiranen, T., Kuva, J., Välimaa, J., 2019. A succession of near-orthogonal horizontal tectonic shortenings in the Paleoproterozoic Central Lapland Greenstone Belt of Fennoscandia: constraints from the world-class Suurikuusikko gold deposit. Mineralium Deposita 55, 1605–1624. https://doi.org/10.1007/s00126-019-00910-7

Sibson, R.H., Robert, F., Poulsen, K.H., 1988. and Mesothermal Gold-Quartz Deposits. Geology 16, 551–555.

Smeds, H., 2015. Location and paragenesis of gold and sulfide phases at the Iso-Kuotko gold prospect, northern Finland.

Ward P, Härkönen I, Nurmi PA, Pankka HS, 1989. Structural studies in the Lapland greenstone belt, northern Finland, and their application to gold mineralization. Geological Survey of Finland, Special Paper 10.

Wyche, N.L., Eilu, P., Koppström, K., Kortelainen, V., Niiranen, T., Välimaa, J., 2015. The Suurikuusikko gold deposit (Kittilä Mine), northern Finland. In: Maier, W.D., Lahtinen, R., O'brien, H. (Eds.), Mineral Deposits of Finland. Elsevier, Amsterdam.

Calculated vein densities from drill core box images. Not applicable for precise interpretation, but they display the true amount of veins per meter vs vein densities displayed in results. In each diagram Y axis displays depth as meters (MD) and X axis displays veins per meter.

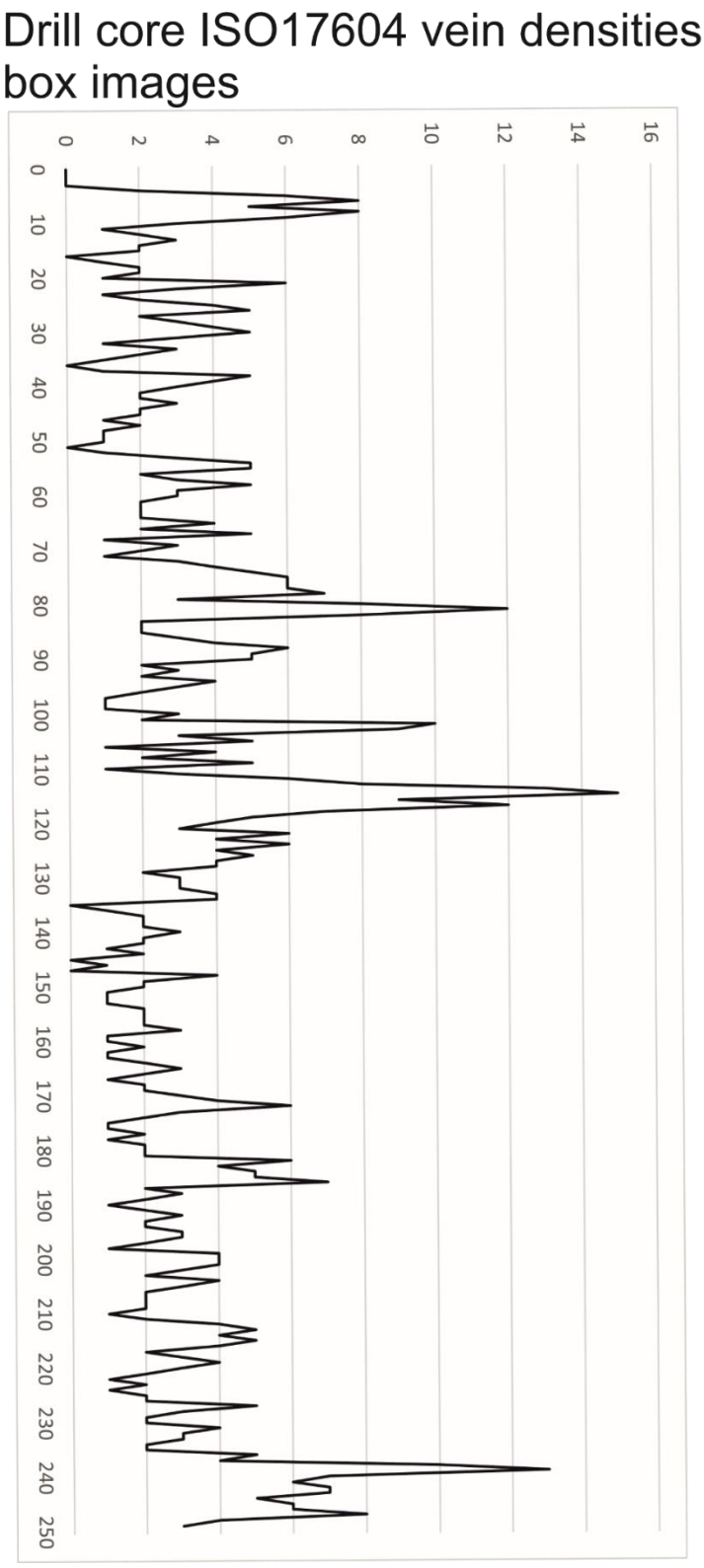

Drill core ISO17605 vein densities from drill core box images

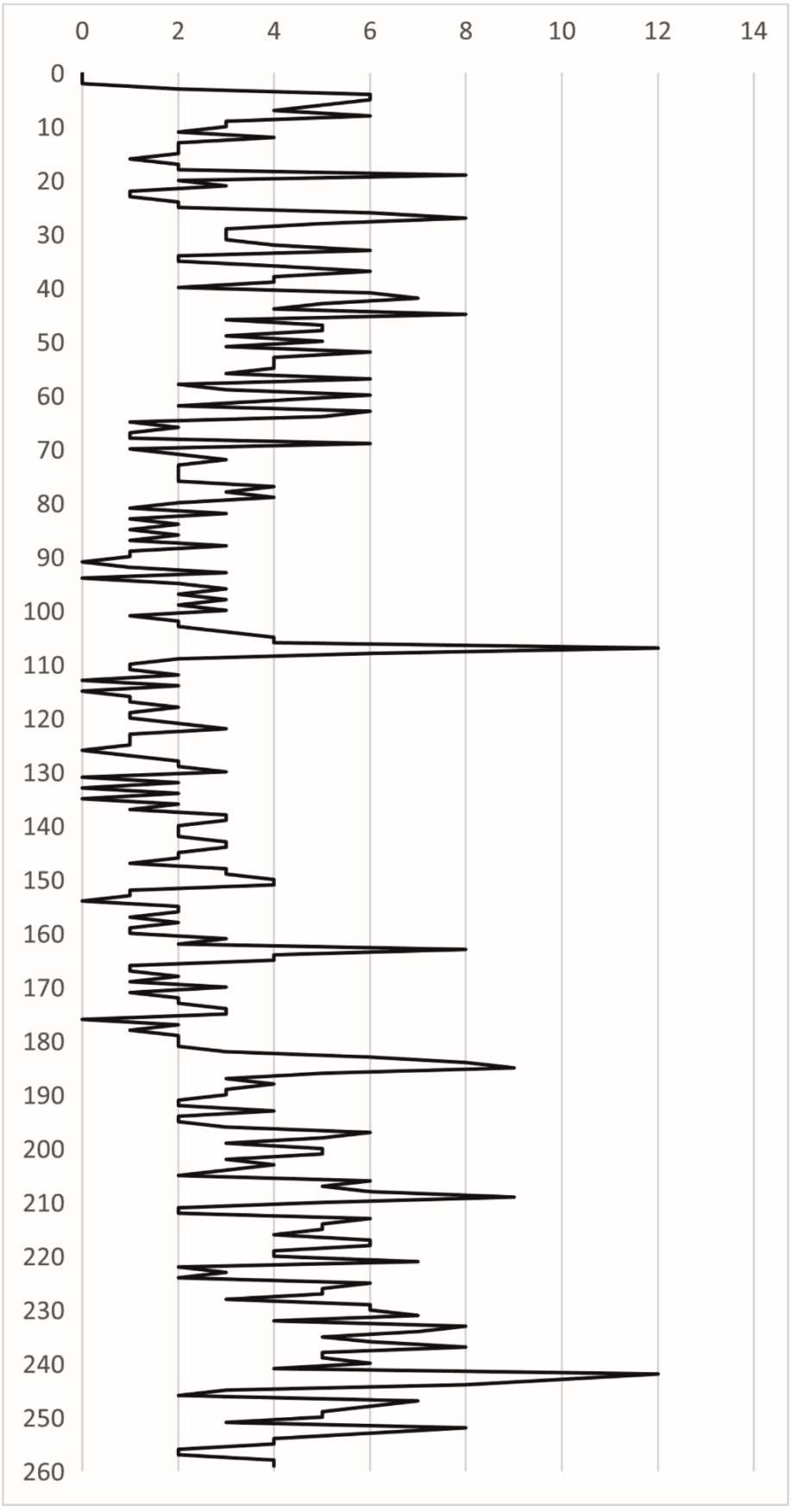

Drill core ISO17609 vein densities from drill core box images

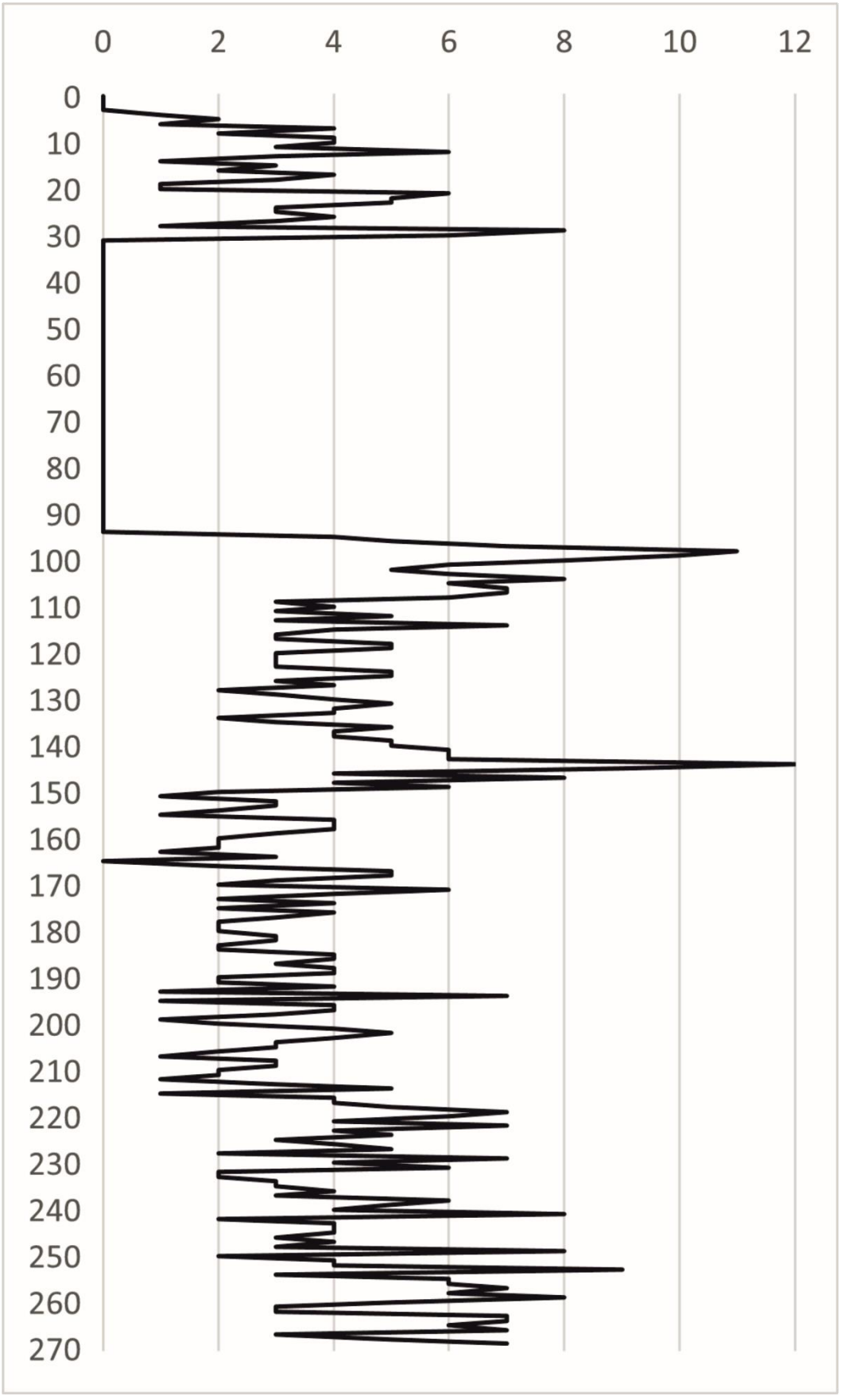

Drill core ISO18602 vein densities from drill core box images

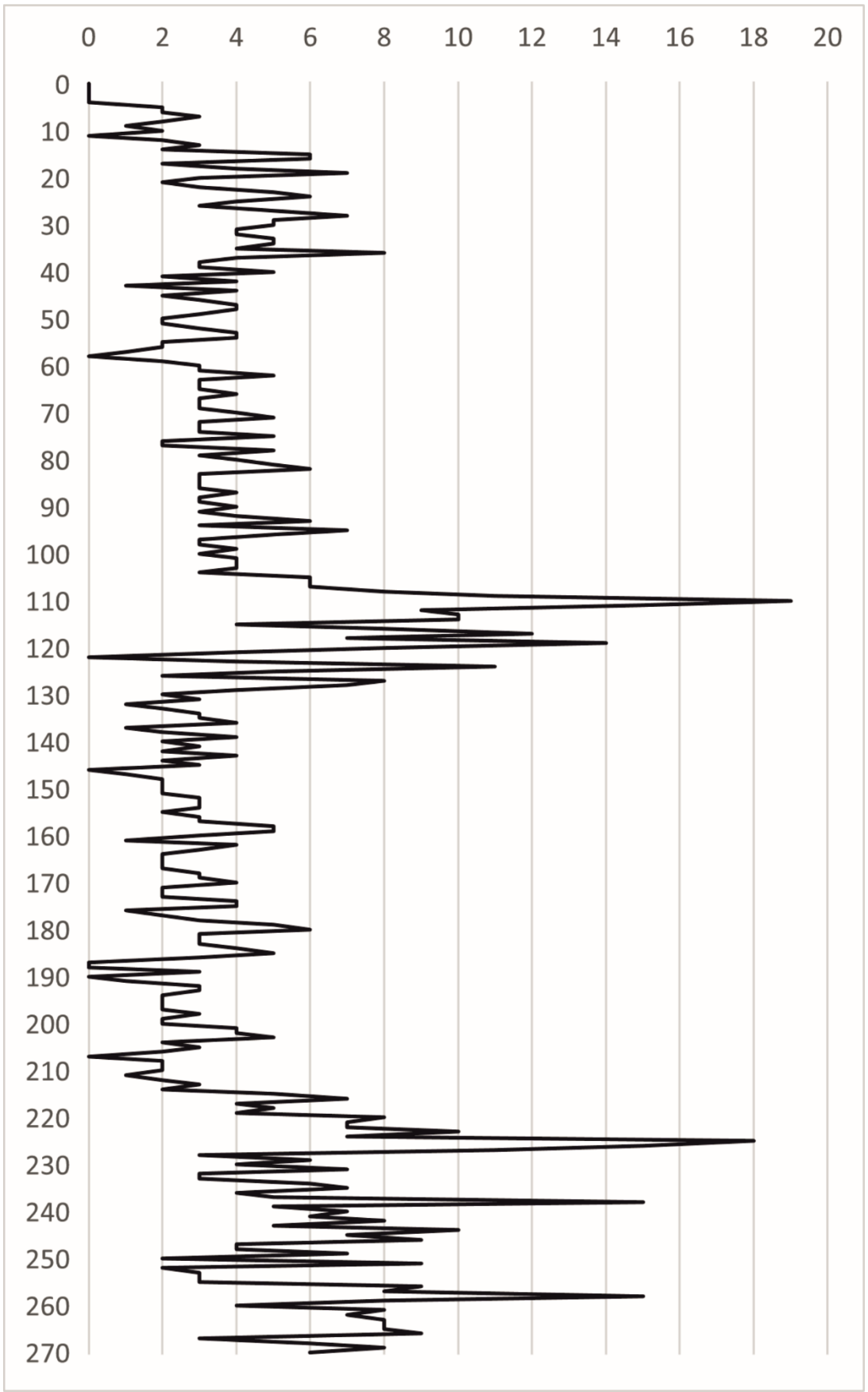

Drill core ISO18603 vein densities from drill core box images

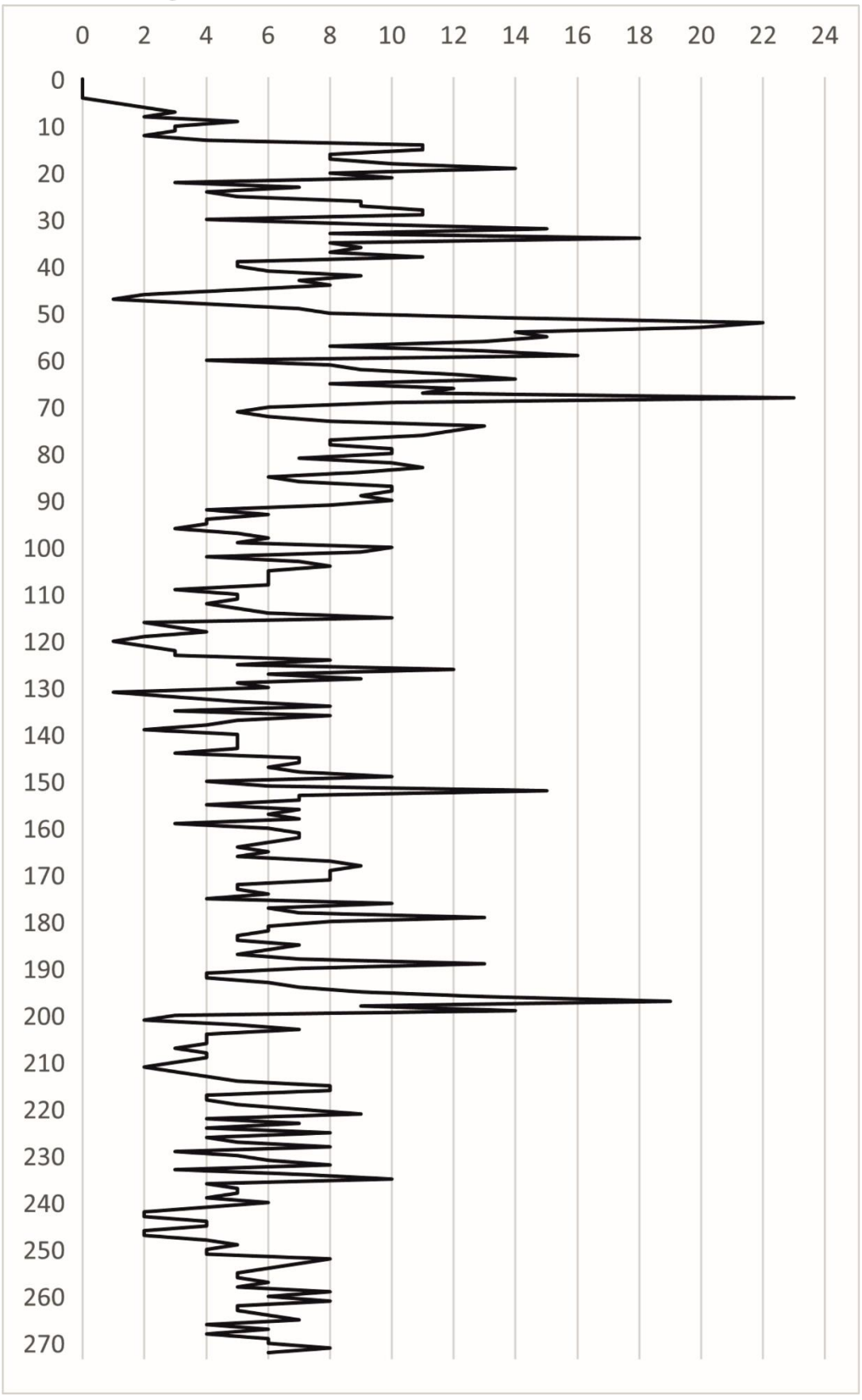

Drill core ISO21004 vein densities from drill core box images

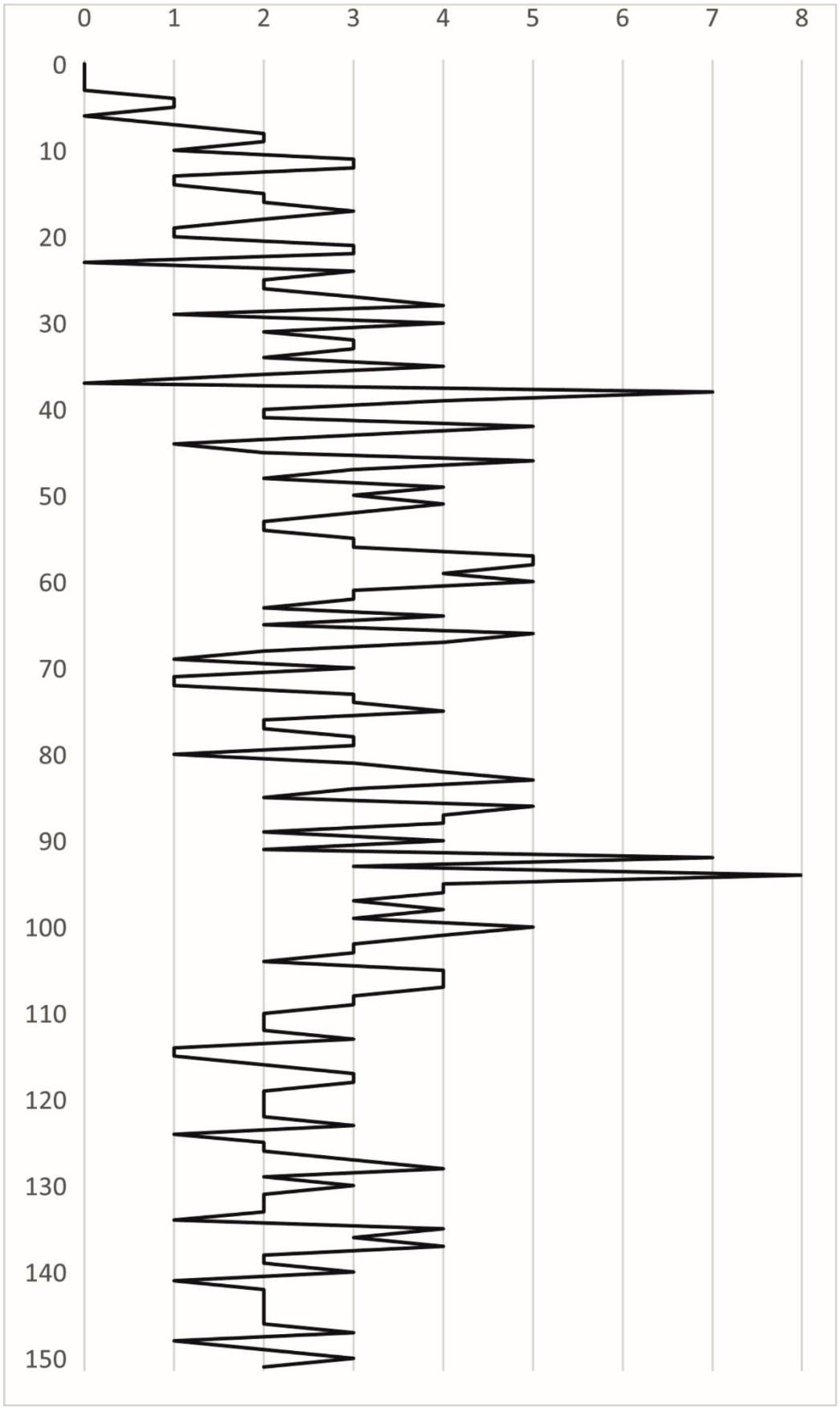

Drill core ISO21006 vein densities from drill core box images